4

Combustion of Energetic Materials

Richard A. Yetter
Penn State University

Princeton-Combustion Institute
2018 Summer School on Combustion
June 25-29, 2018
Princeton, NJ

Chemical Kinetics and Flame Structure of Energetic Materials

What are molecular and homogeneous energetic materials

- These are the “premixed” systems of energetic materials
  - Kinetically limited, not diffusion
- Monomolecular (single molecular)
  - Pure materials and plastic bonded
    - Small amount of binder is neglected
- Molecularly mixed materials
  - Double based and triple base

Aliphatics

- Aliphatic organic compounds belong to the alkane, alkene, and alkyne classes of compounds
- Both open chained and cyclo aliphatic groups
- The major sources of oxidizer are from the nitro ($-NO_2$), nitrite (-ONO), nitrate ($-ONO_2$), and nitramine ($-NH-NO_2$) groups

Nitromethane

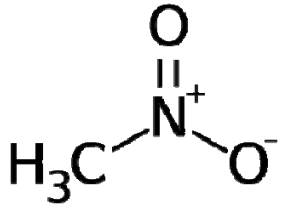

Methylnitrite

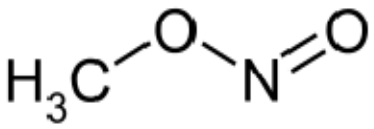

Methylnitrate

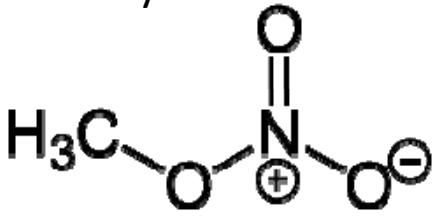

Nitroglycerine, NG

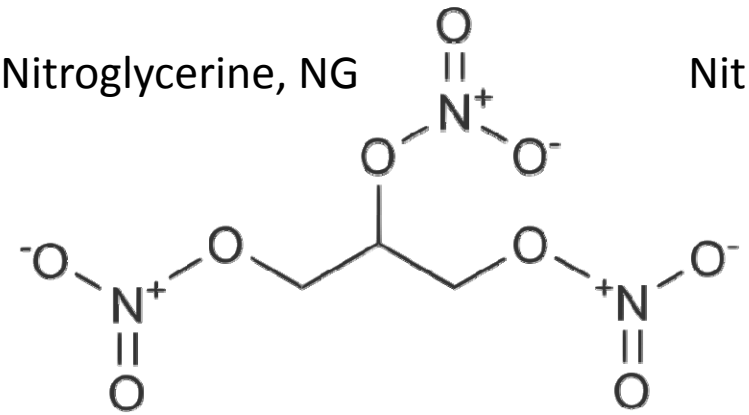

Nitroguanidine, NQ

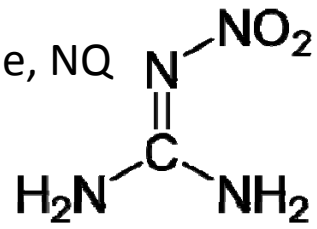

Pentaerythritoltetranitrate, PETN

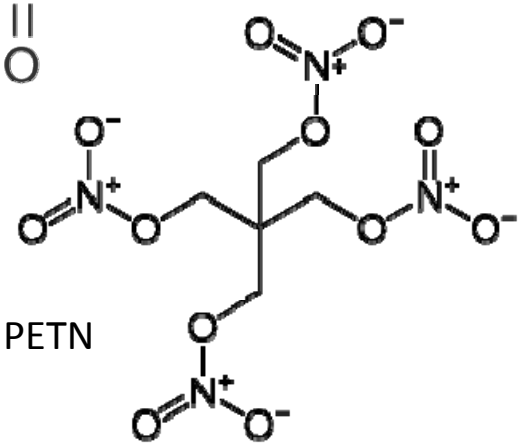

Cycloaliphatics

- These are also nitramines
- Very commonly used in propellants and explosives
- They are really not flat. In fact, they can have different configurations, which give different crystal structures, which are different solid phases

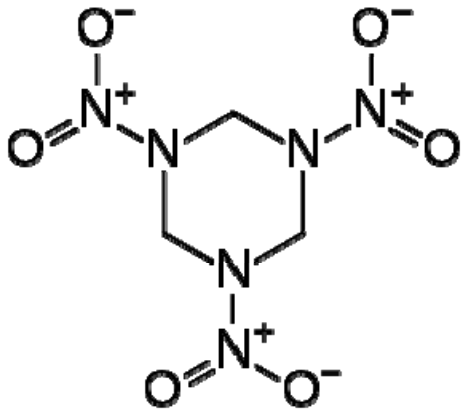

Cyclotrimethylene
Trinitramine, RDX

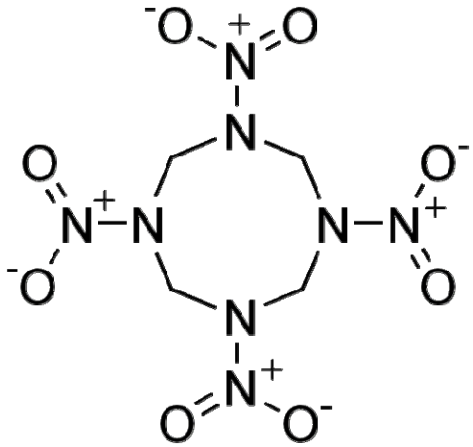

Cyclotetramethylene
Tetranitramine, HMX

Aromatics

- Oxygen added by -NO_2 groups mainly

Trinitrobenzene, TNB

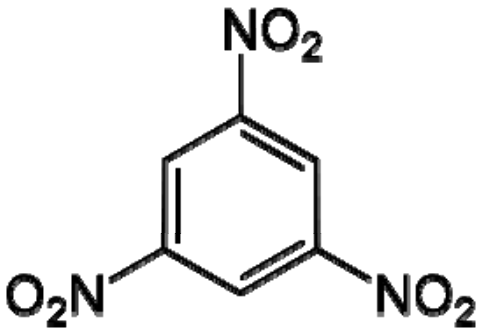

(Good performance and sensitivity, but difficult to make - expensive)

Trinitrotoluene, TNT

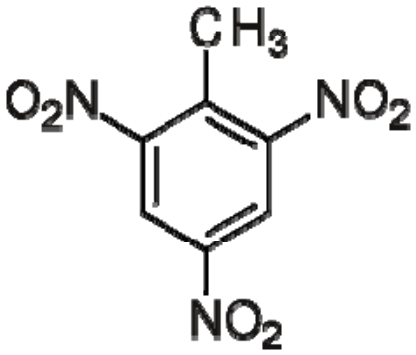

Triaminotrinitrobenzene, TATB

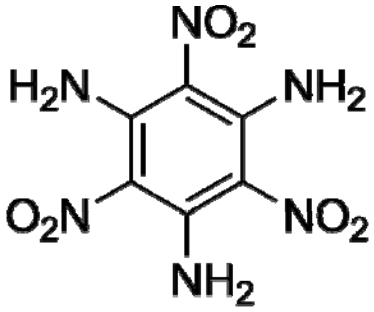

(The standard for insensitivity)

Trinitrophenol, Peric Acid

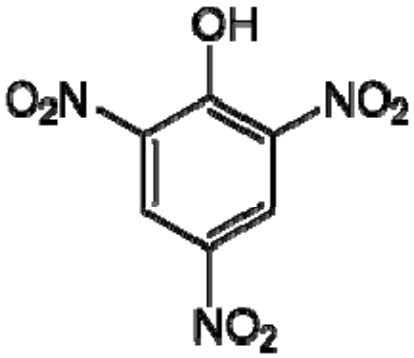

Lead styphnate

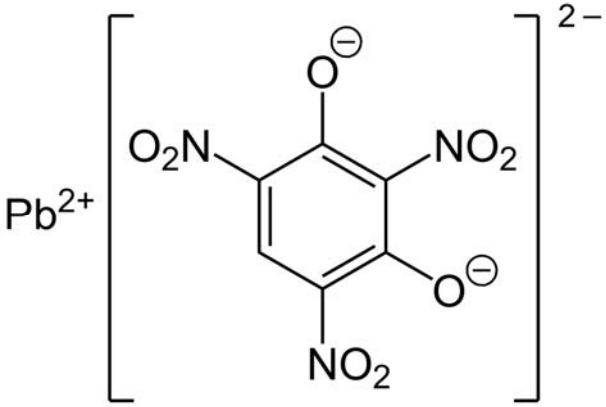

Inorganics

- Inorganic compounds do not have hydrocarbon backbones forming the basis of the molecules
- Usually are ionic acids or bases, or salts

Ammonium nitrate, AN, $NH_4^+NO_3^-$

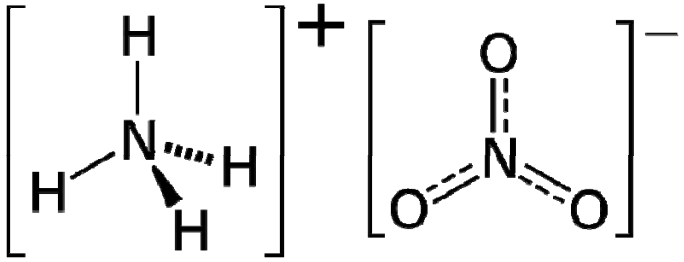

(hard to use as a propellant or explosive, but very inexpensive, and chlorine free)

Ammonium perchlorate, AP, $NH_4^+ClO_4^-$

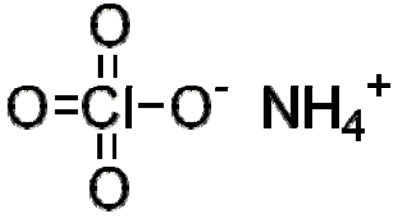

(common composite propellant oxidizer)

Also azides, e.g., lead azide

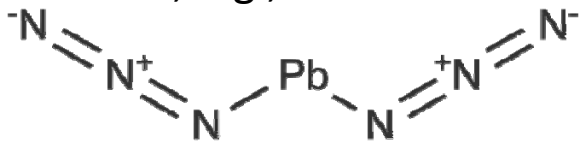

Potassium chlorate, $KClO_3$

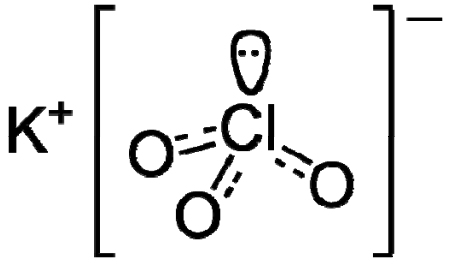

(no oxidizer surpasses its burning speed and ease of ignition, becomes sensitive with red phosphorous, can decompose under UV)

Potassium perchlorate, $KClO_4$

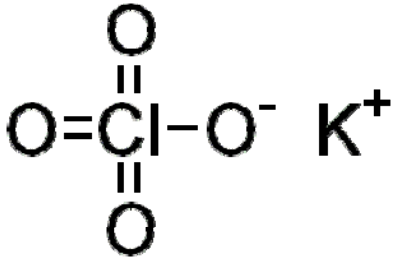

(can explode alone with strong impact, less prone to decompose under UV than $KClO_3$)

Some Newer Energetic Materials

Ammonium dinitramide, ADN

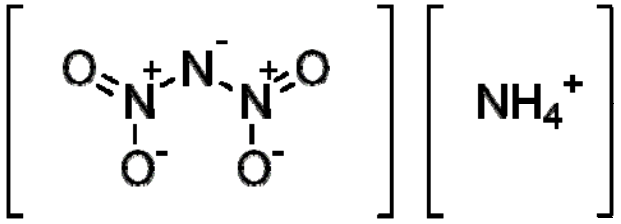

Hydroxylammonium nitrate, HAN, NH_3OHNO_3

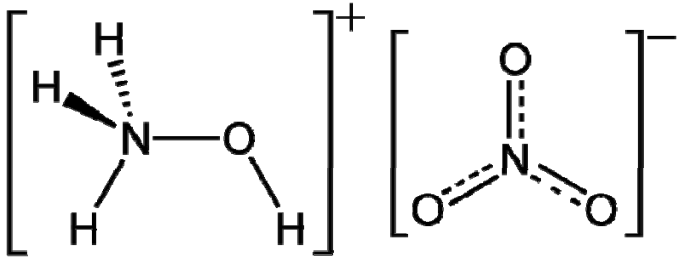

5-Nitro-1,2,4-triazol-3-one, NTO

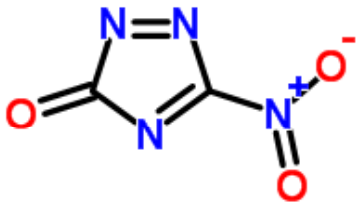

1,3,3-Trinitroazetidine, TNAZ

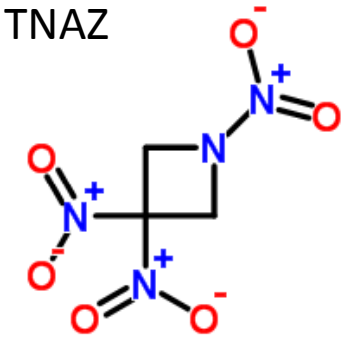

2,4,6,8,10,12-Hexanitro-2,4,6,8,10,12-hexa-azatetracyclododecane, CL-20

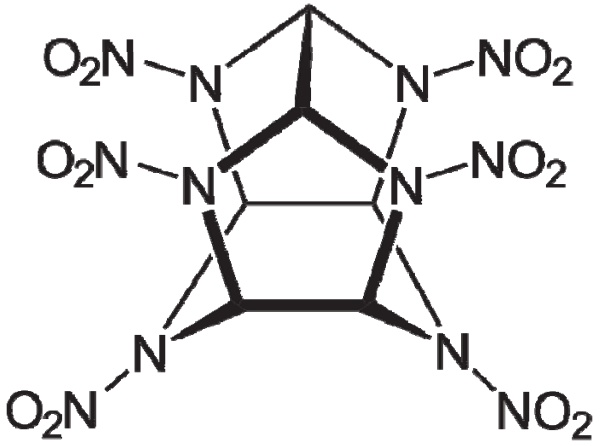

Octanitrocubane

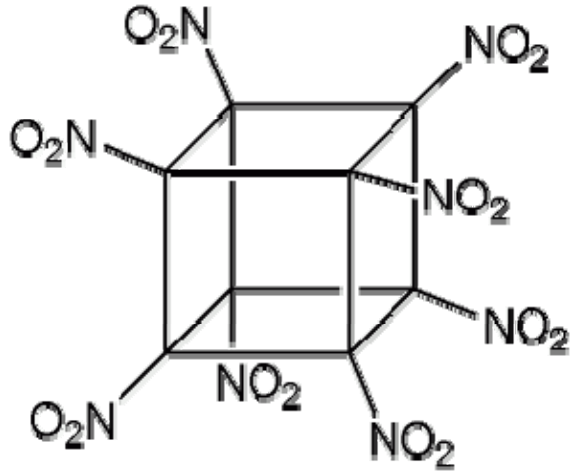

High-Nitrogen Energetic Materials

Focus is on HN ring systems with *known* chemistries

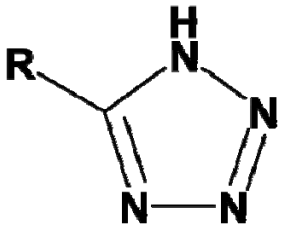

tetrazole

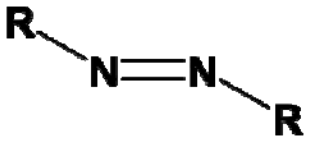

azo

azide

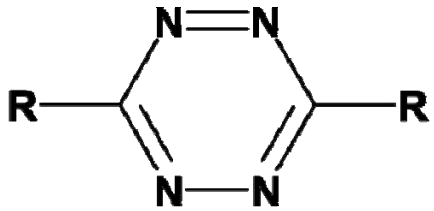

tetrazine

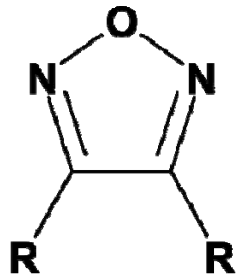

furazan

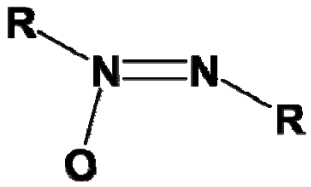

azoxy, N-oxide

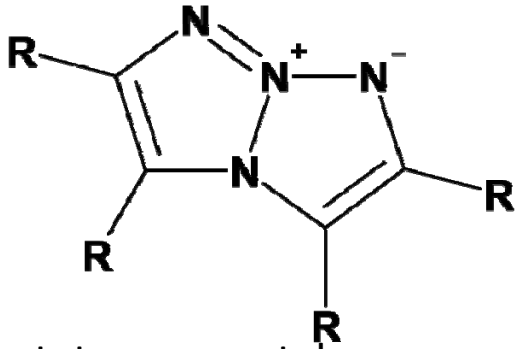

tetraaza pentalene

High-Nitrogen Energetics Exhibit Unusual Properties

- Explosive Performance vs Sensitivity rule does not follow.
  AAzF, DAAF
- High Burn Rates with Low Pressure Sensitivity
  (DAATO3.5, 100 atm, 6 cm/s, n=0.275)
- Detonate despite having no oxygen
  DHT/DAAT
- Burn rapidly without visible flame
  DHT/BTATz
- High Hydrogen also
  DHT/TAGzT

DAAF

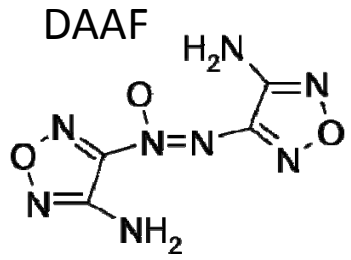

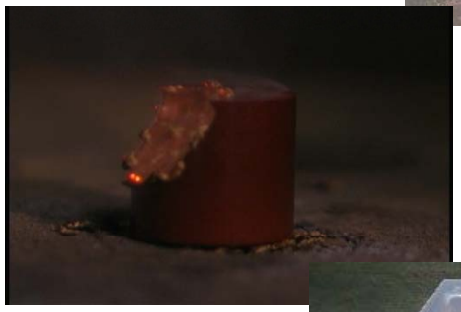

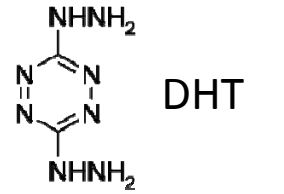

DHT

BTATz

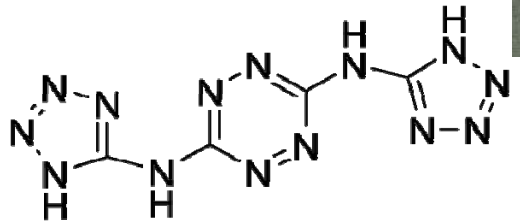

Reactions and Energetics of Decomposition

- Simple bond fission

  $BDE = \Delta H^0_{f,298}(A) + \Delta H^0_{f,298}(B) - \Delta H^0_{f,298}(A-B)$

  BDE (C–NO_2) > BDE(C–NO), BDE(N–NO_2) ~ BDE(N–NO)

  BDE(C–NO_2) ~ BDE(C–ONO), BDE(N–NO_2) >BDE(N–ONO)

  By comparing bond strengths, one finds CH_3ONO and CH_3ONO_2 decompose by breaking the O-N bond rather than the C-O bond

- Bond fission of radicals

  Energy required to break a bond in a radical species can differ from the BDE – must consider a barrier to dissociation in addition to the BDE

  The BDE for removing the radical species from a radical adduct generally less than the corresponding BDE for the stable species

- Concerted decomposition

  Alternative decomposition process is a concerted process in which the activation energy is lower than any of the individual bonds

  Trioxane 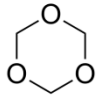 $(-CH_2O-)_3 \rightarrow 3\,CH_2O$; $RDX \rightarrow 3\,CH_2NNO_2$

- Complex fission – five centered HONO elimination
- Autocatalytic- radical attack on energetic materials
- Water assisted reactions

Bond Dissociation Energies for Various Nitro, Nitroso, Nitrite, and Nitrate Species in kcal/mol

Nitroso Compounds	
H–NO	50.3
CH3–NO	37.6
NH2–NO	49.4
HO–NO	50.2
CH3O–NO	43.5
CH2H–NO	22.1
CH3NH–NO	48.7
CH2CH–NO	51.0
C2H5-NO	38.5
NH2CHCH–NO	60.6
CHO–NO	29.2
NH2O–NO	17.1
HOO–NO	25.5
CH3NHO–NO	12.1
CH2CHO–NO	15.5

Nitro Compounds	
H–NO2	73.4
CH3–NO2	58.9
NH2–NO2	51.4
HO–NO2	46.8
CH3O–NO2	39.9
CH2H–NO2	37.1
CH3NH–NO2	50.6
CH2CH–NO2	70.2
C2H5-NO2	60.8
NH2CHCH–NO2	78.2
CHO–NO2	49.8
(CH3)2N–NO2	45.9
NH2CHCH–NO2	78.2

Nitrite Compounds	
H–ONO	78.3
CH3–ONO	57.3
NH2–ONO	32.9
HO–ONO	17.1
CH3NH–ONO	29.3
(CH3)2N–ONO	28.1
CH2N–ONO	22.1
CH2CH–ONO	68.5
C2H5-ONO	59.3
CHO–ONO	60.0

Nitrate Compounds	
H–ONO2	105.0
CH3–ONO2	83.7

From Melius, 1989

Comparison of decomposition energetics of NO_2 bond breaking and HONO elimination for CH_3ONO_2, CH_3NHNO_2, $CH_3CH_2NO_2$, and $CH_2{=}CHNO_2$

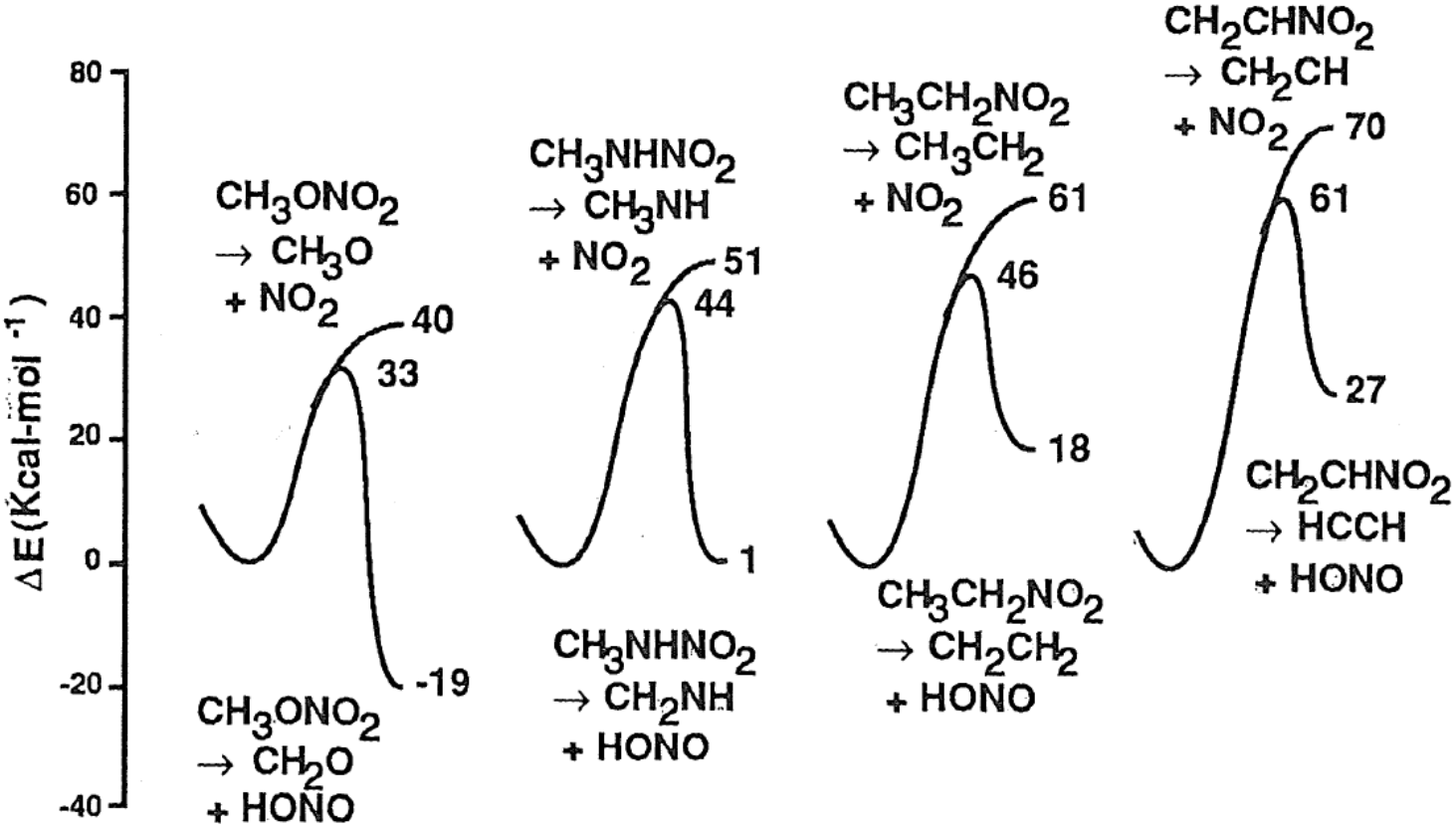

- The top energy value represents the bond dissociation energy for NO_2 bond fission
- The middle energy value represents the barrier height for the 5-centered elimination of HONO
- The bottom energy represents the heat of dissociation for formation of HONO

Reaction of CH_3NHNO_2 + H

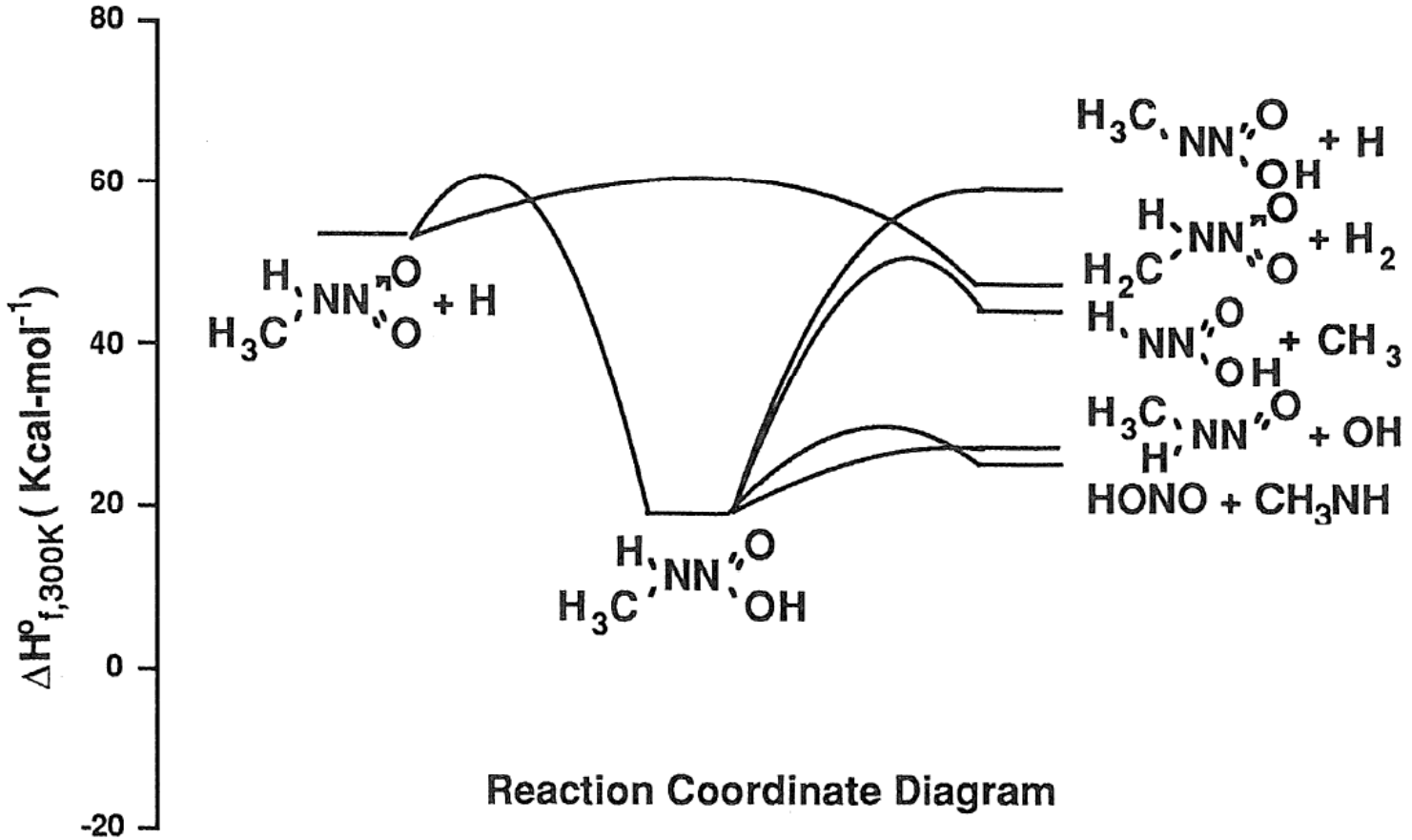

From Melius, 1989

Reaction diagrams for the water catalyzed concerted reaction for the conversion of nitramine, NH_2NO_2, to N_2O+H_2O through the intermediate *aci* form, HNN(O)OH

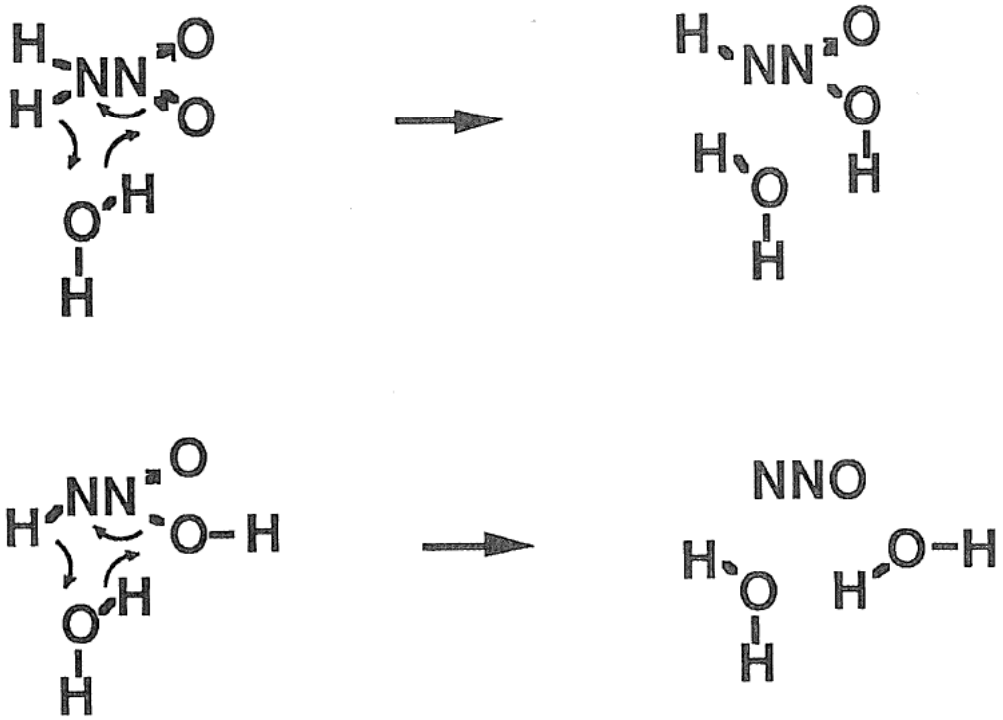

- In the first concerted mechanism, the H from the nitramine shifts to the water molecule while the H on the water shifts to the O of the nitramine, forming the *aci* molecule
- In the second step, the *aci* molecule is converted to N_2O and H_2O by again having the H bonded to the N shifting to the water molecule while the H on the water molecule is shifted to the OH group of the *aci* molecule

From Melius, 1989

Gas-Phase Experiments and Model Development

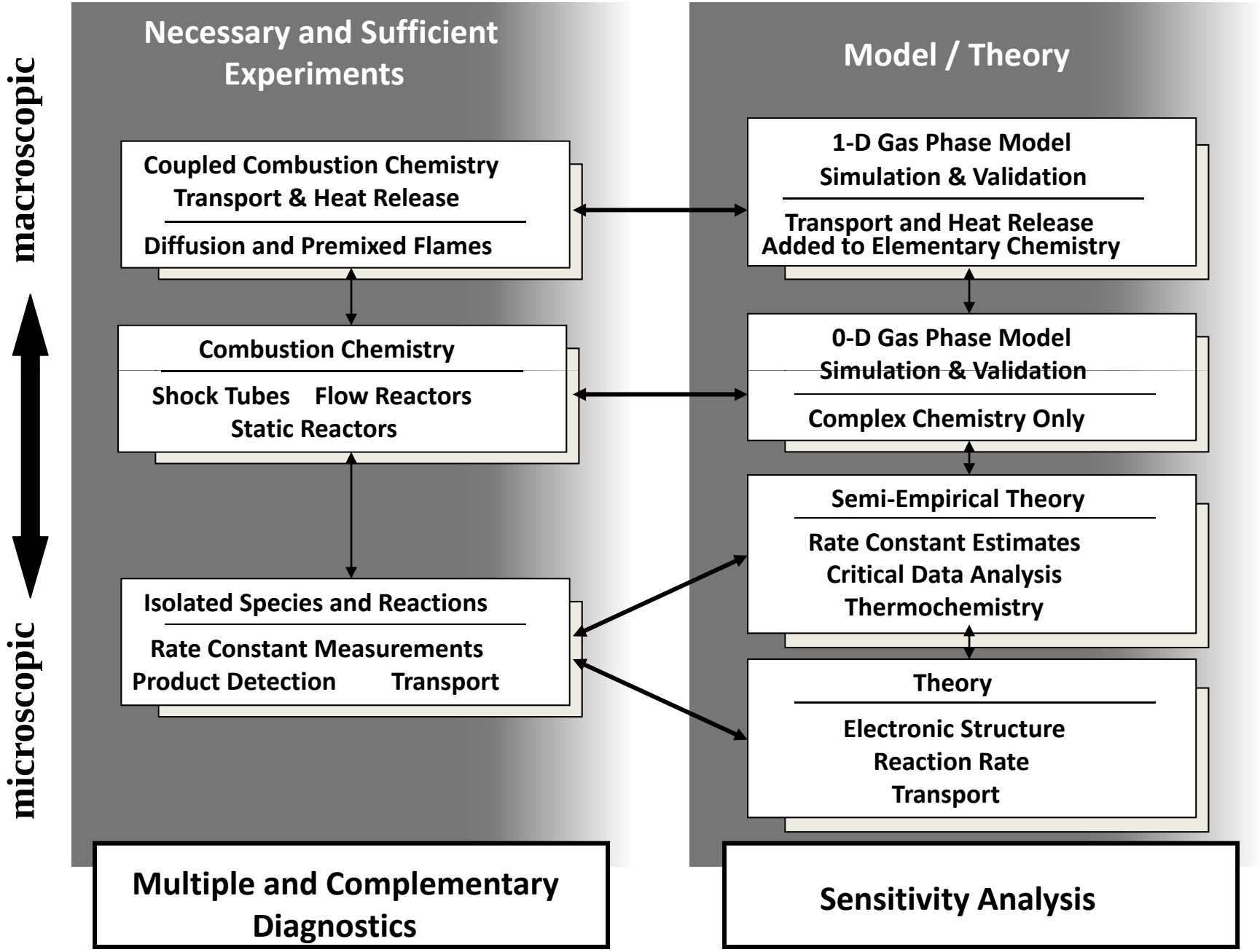

Gas-Phase Chemistry Mechanisms

Hydrocarbon Combustion Chemistry

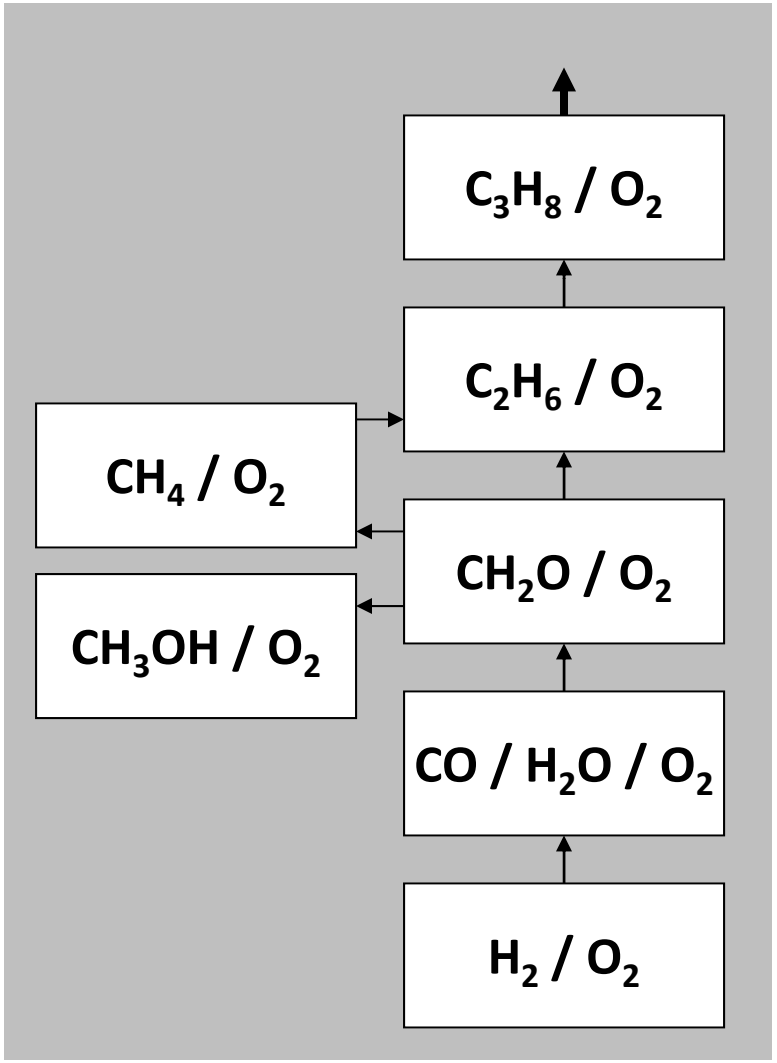

Nitrate Ester / Nitramine Combustion Chemistry

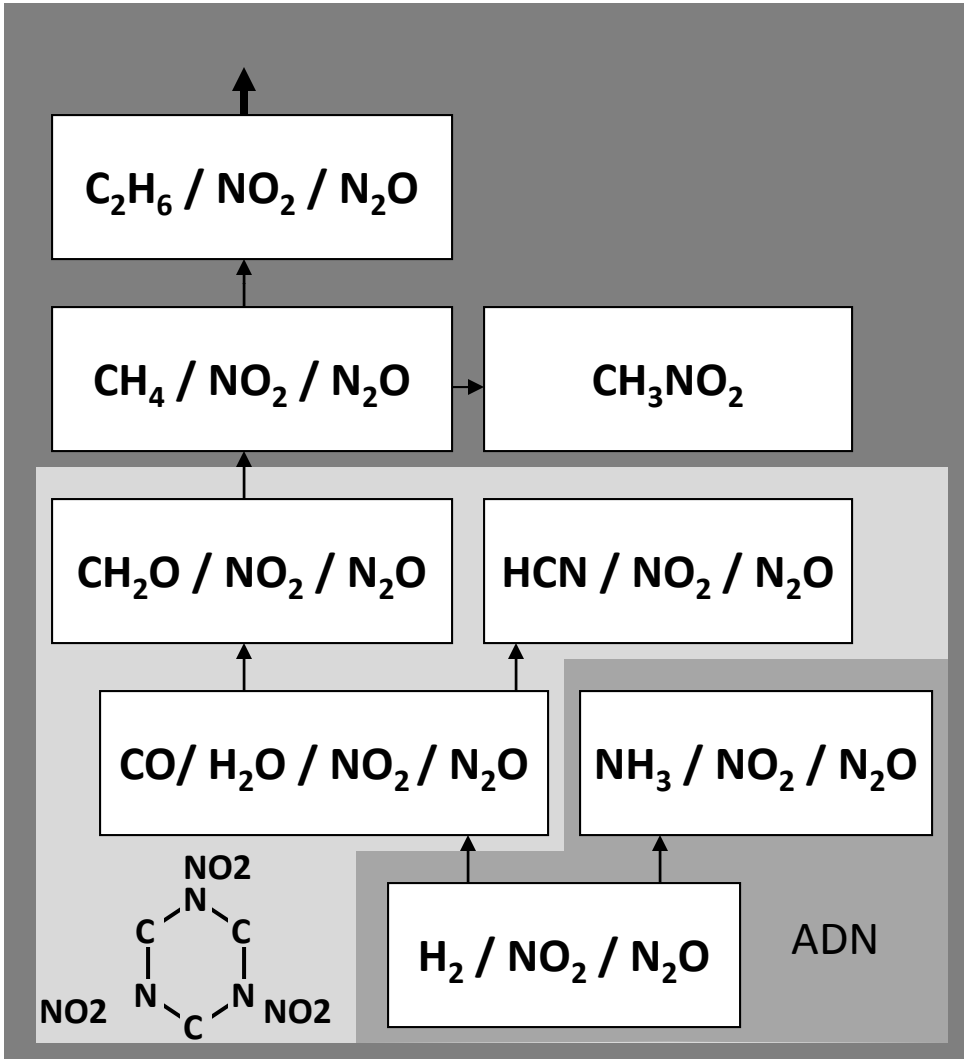

Gas-Phase Submodel Development

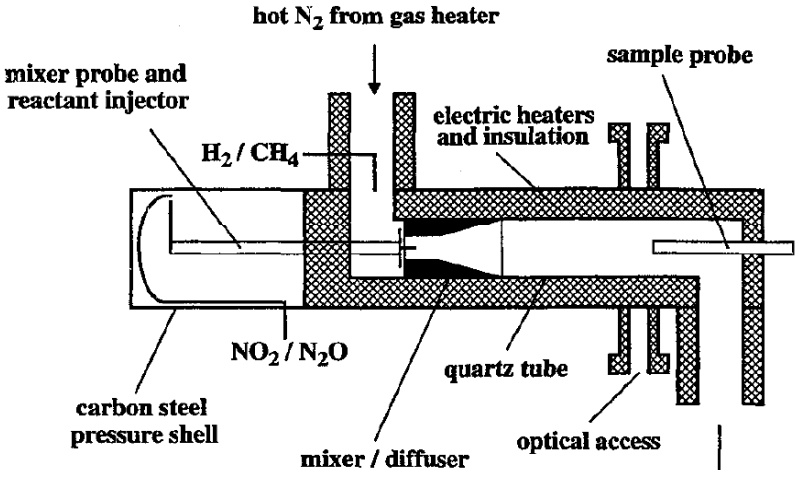

Flow reactor studies of N_2O decomposition at 6 atm and 1123 K

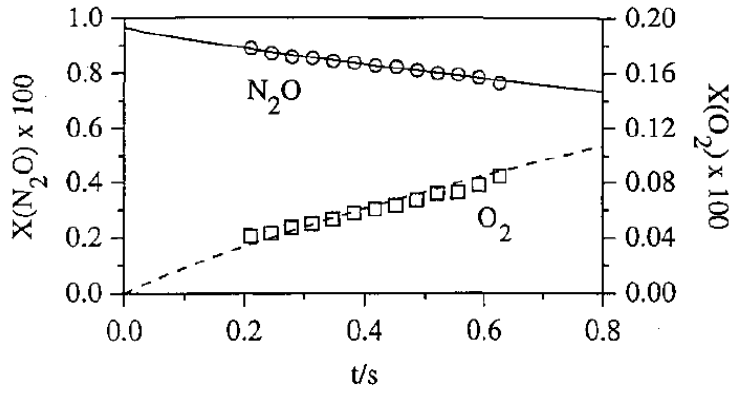

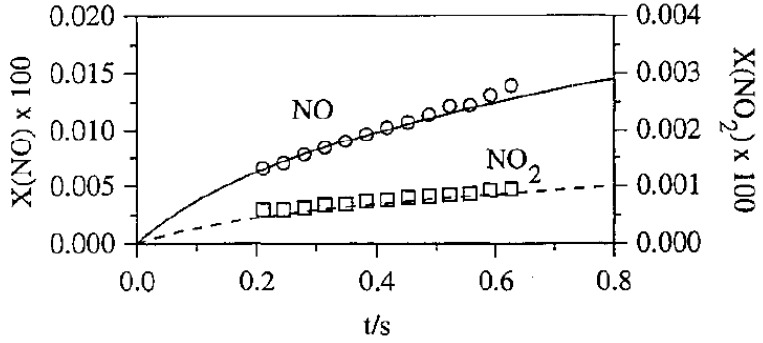

Flow reactor studies of a $CH_4/N_2O/N_2$ mixture reacting at 3.3 atm and 1153 K

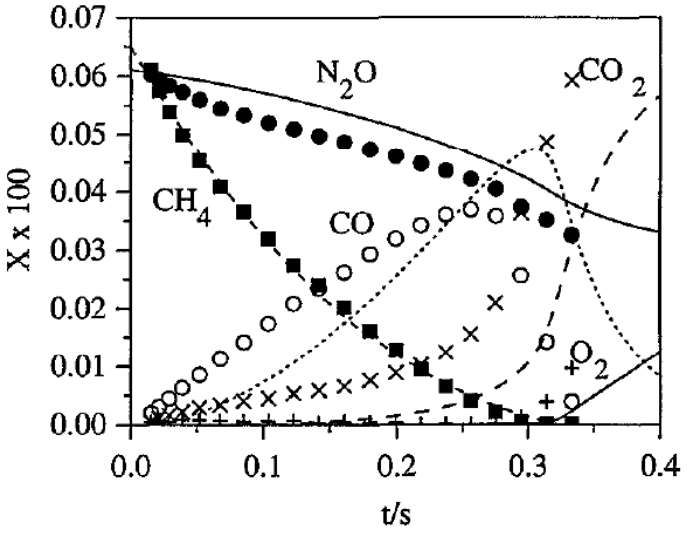

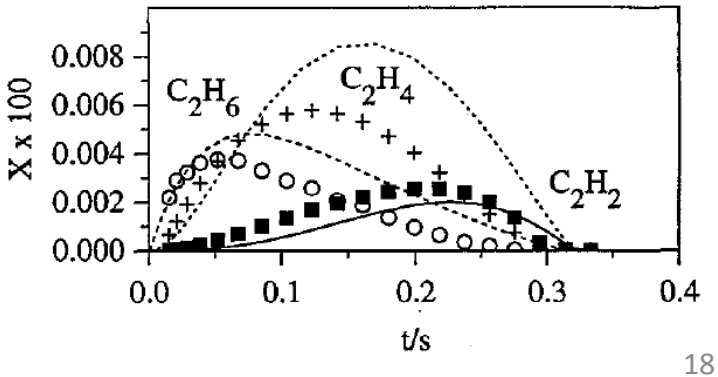

Constant Volume Nitromethane Combustion - Temperature

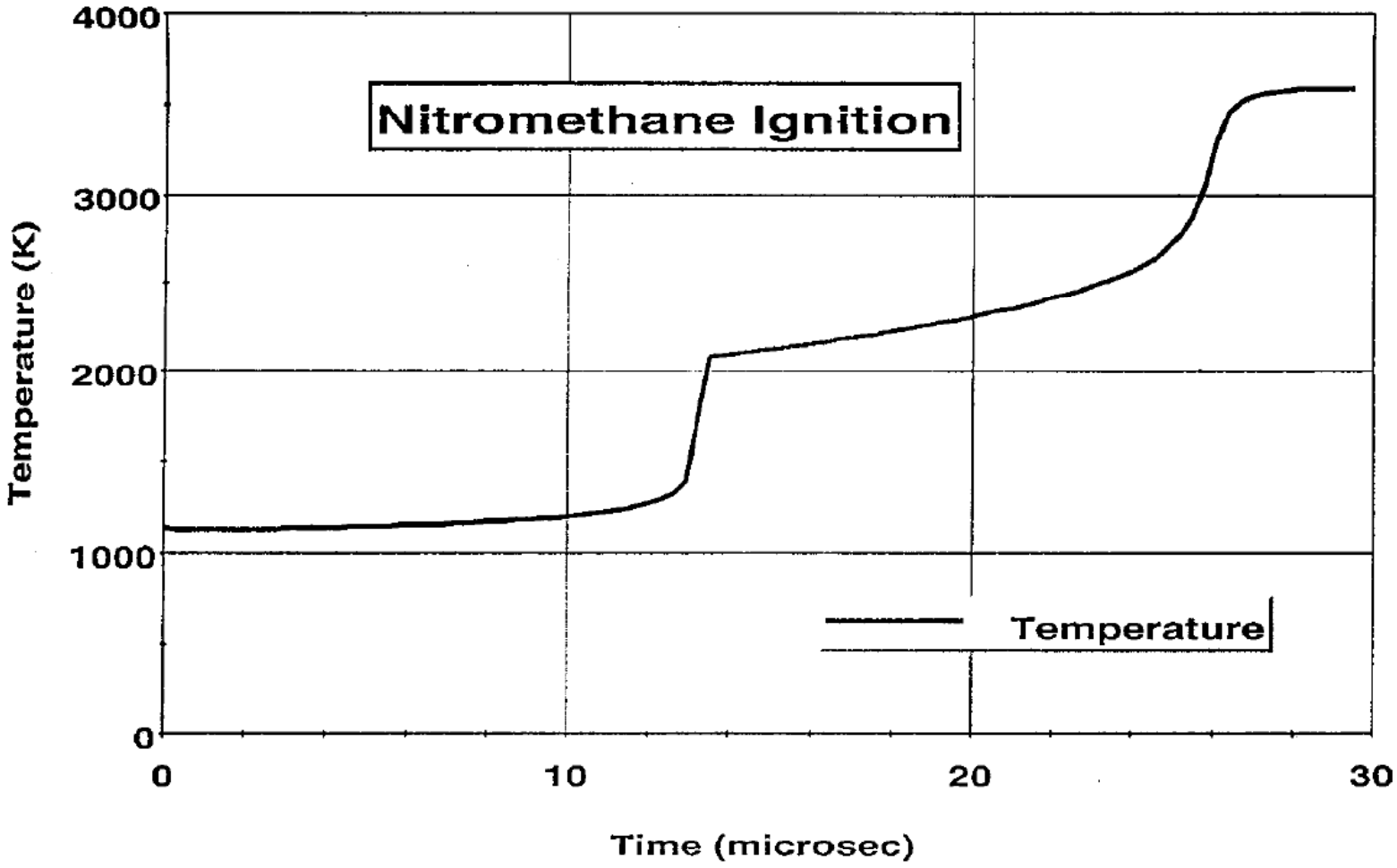

Initial Conditions: 100% gaseous CH_3NO_2, T_i = 1100 K; P_i = 7.25 atm

From Melius, 1995

Constant Volume Nitromethane Combustion - Species

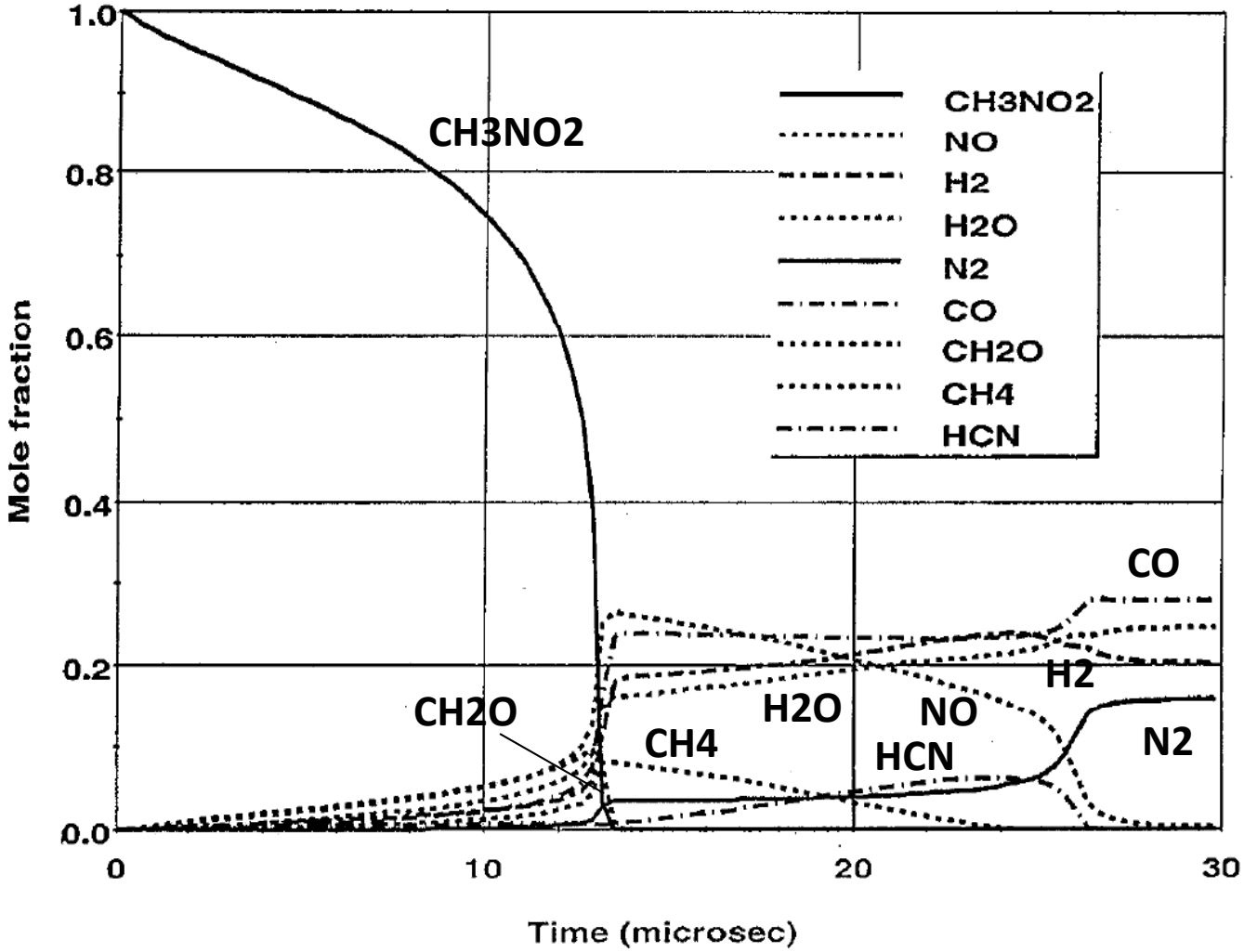

Initial Conditions: 100% gaseous CH_3NO_2, T_i = 1100 K; P_i = 7.25 atm

From Melius, 1995

Nitromethane First Stage Chemistry

Carbon Mechanism

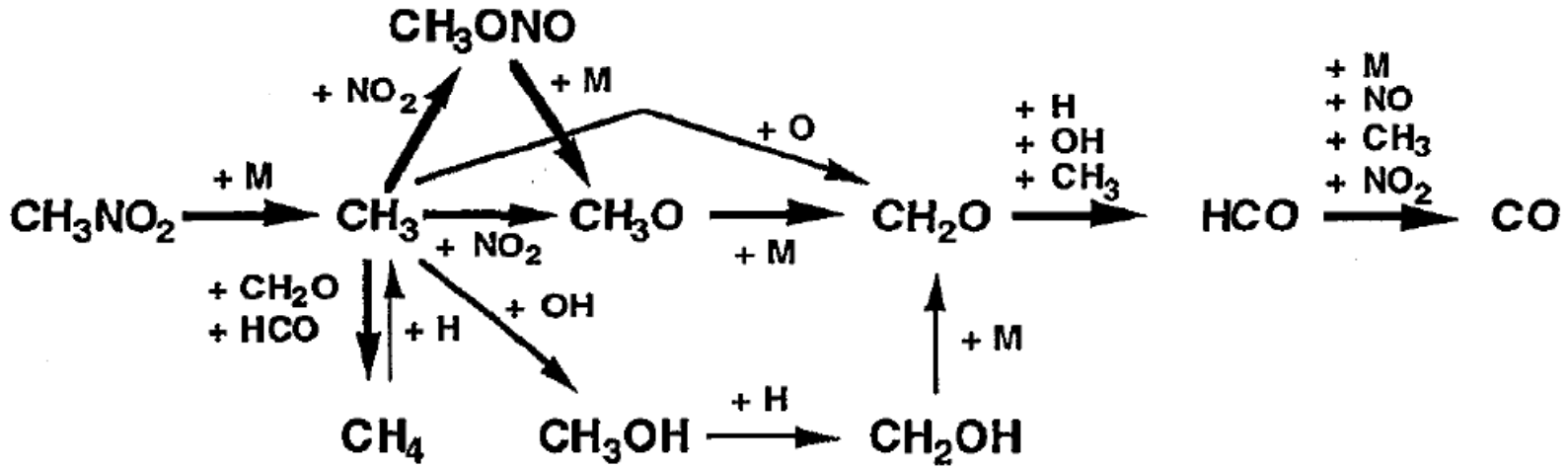

Nitrogen Mechanism

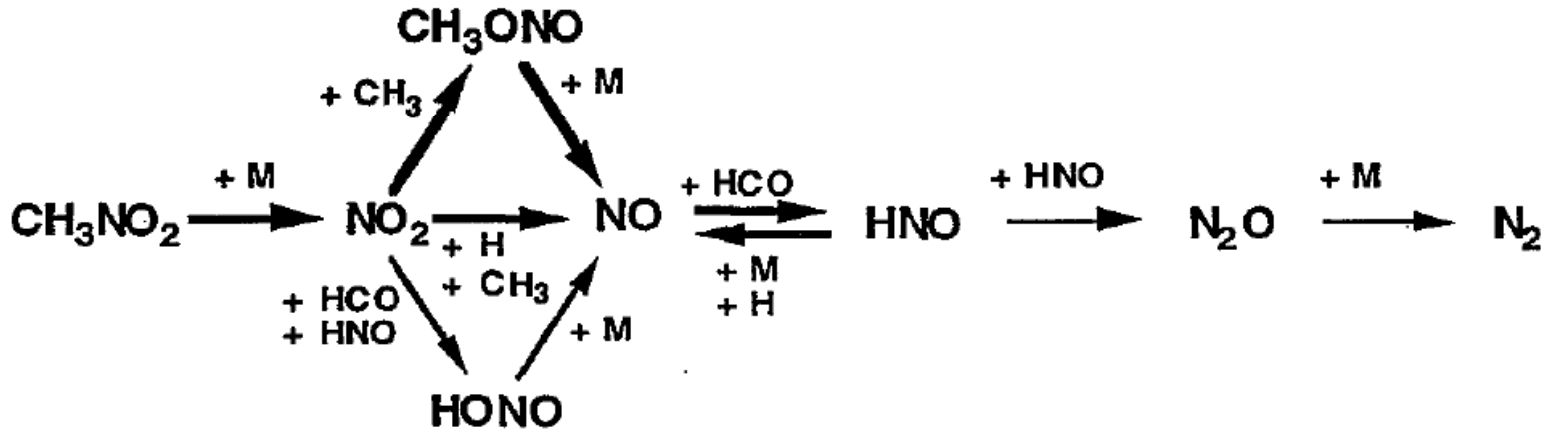

From Melius, 1995

Nitromethane Intermediate (Dark Zone) Stage Chemistry

Carbon Mechanism

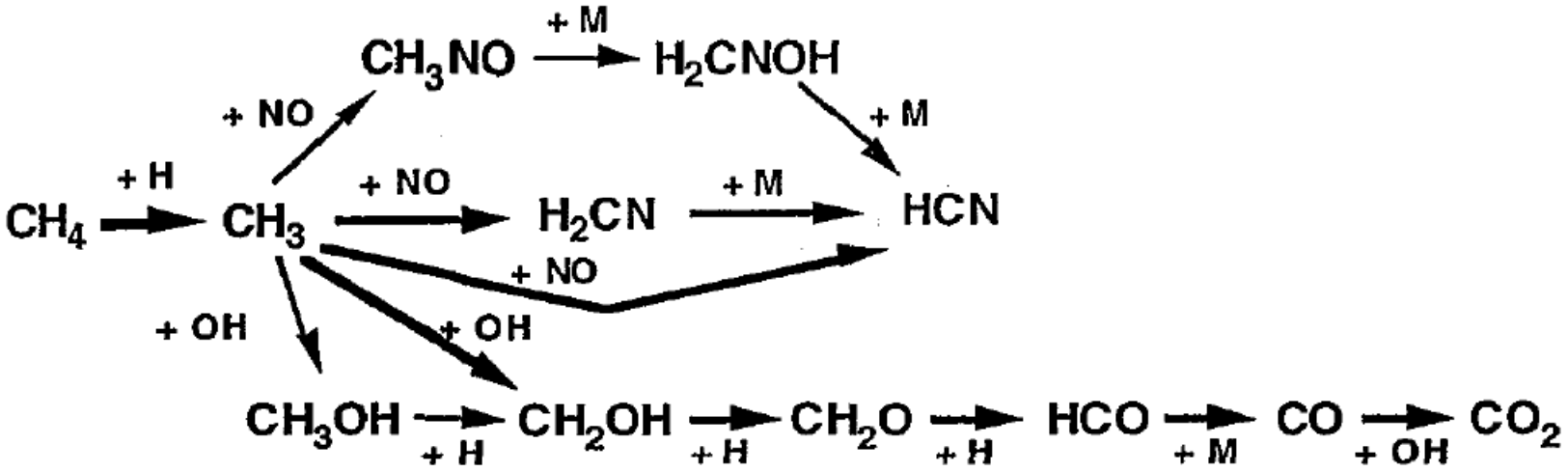

Nitrogen Mechanism

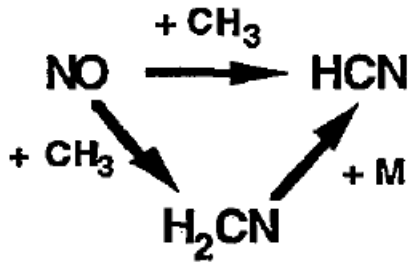

From Melius, 1995

Nitromethane Second Stage Chemistry

Carbon Mechanism

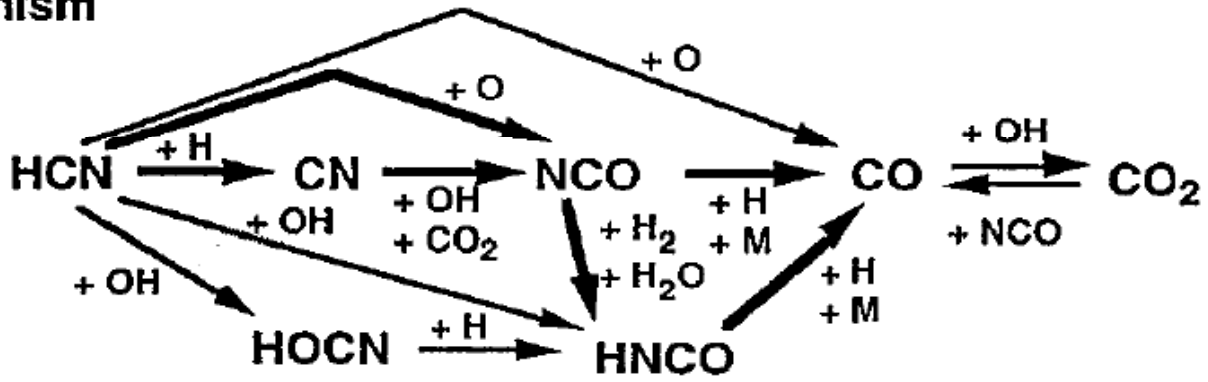

Nitrogen Mechanism from HCN

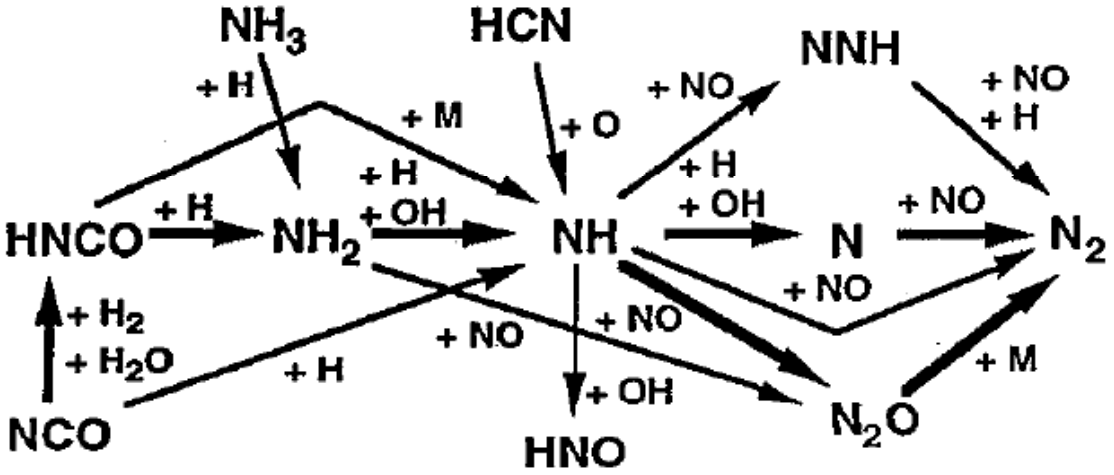

Nitrogen Mechanism from NO

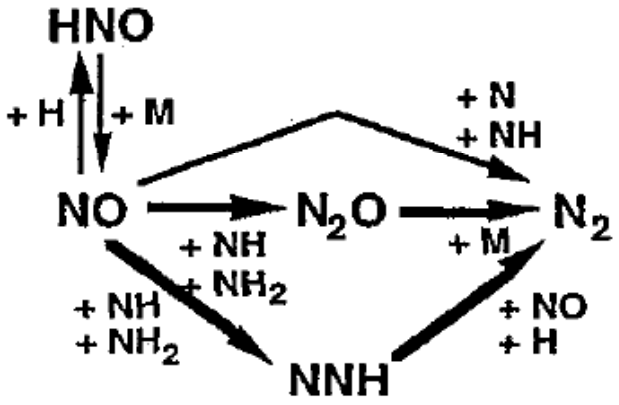

From Melius, 1995

Flame Structure of a Double-Base Propellant

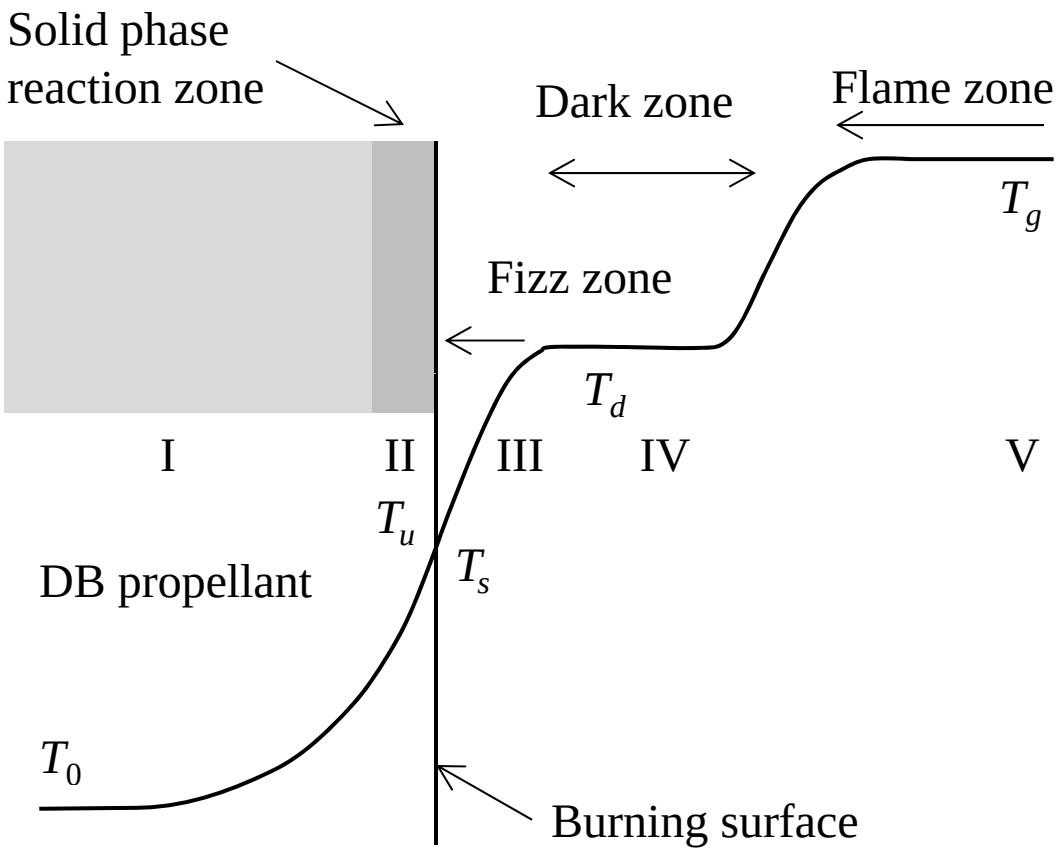

$$RONO_2 \longrightarrow \begin{matrix} NO_2 \\ R'CHO \end{matrix} \longrightarrow \begin{matrix} NO, H_2 \\ CO, CO_2 \end{matrix} \longrightarrow \begin{matrix} N_2, CO \\ CO_2, H_2O \end{matrix}$$

I. **Preheat Zone**: heating of propellant occurs without chemical reaction

II. **Solid-phase reaction zone**: Thermal decomposition begins by CO–NO_2 bond breaking

III. **Fizz Zone**: NO_2 and aldehydes react with other gaseous species to produce NO, CO, H_2, and CO_2

IV. **Dark (induction) zone**: slow oxidation reaction of the products formed from the fizz zone. The dark zone is considered isothermal with nearly negligible thermal and mass diffusion.

V. **Luminous flame zone**: Final products are formed and remainder of heat released

Effect of pressure on flame structure of double base propellant

- As pressure is increased, the rates of reaction in the fizz, dark, and luminous flame zones increase
- The reaction in the dark zone more sensitive to p than the other zones

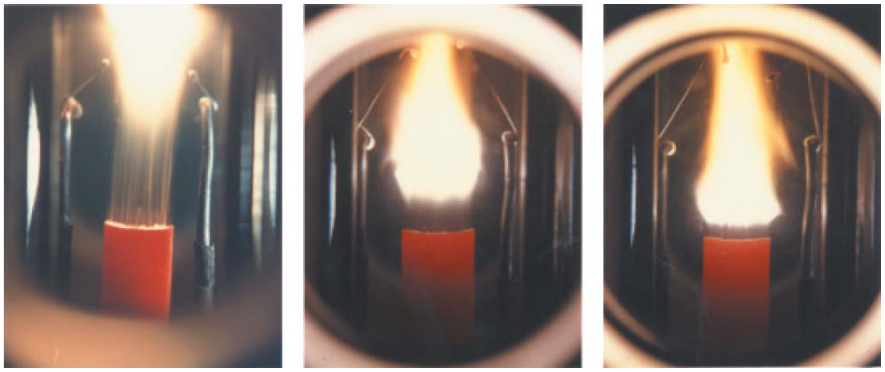

p(MPa)	1	2	3
r_b (mm/s)	2.2	3.1	4.0

From Kubota, Propellants and Explosives, 2002

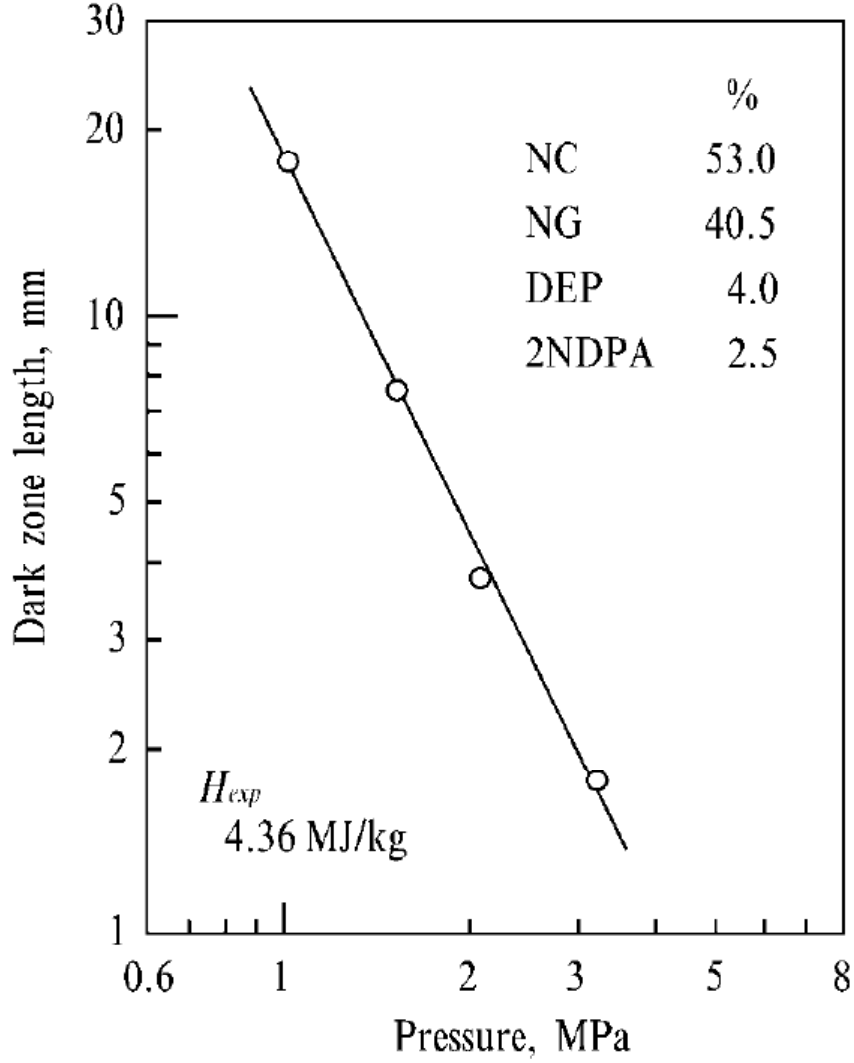

DEP: diethyl phthalate
2NDPA: 2-nitrodiphenylamine

Flame Structure of Double Based Propellants

- Condensed phase mechanisms are often neglected due to the lack of their understanding
- In addition to possible vaporization, initial condensed phase decomposition is assumed to occur at the surface
- A pyrolysis law relates the surface temperature to the rate of reaction, e.g., Zenin (1980) from empirical studies developed the following pyrolysis law for DB propellants

$$\dot{m}''\left(\mathrm{g/m^2}-s\right)=1.8\times10^3\,exp\left(-\frac{5000}{T\left(K\right)_s}\right)=r_b\rho_p$$

- Various types of thermolysis experiments where the surface is heated in a low temperature (and often low pressure) gas environment are used to measure the species composition evolving from the surface

Flame Structure of Double Based Propellants-cont'd

- The condensed phase of very few simple ingredients, such as RDX, and a few simple binary mixtures, have been studied
- Detailed gas-phase processes, including complex elementary reaction mechanisms, heat transfer, and multicomponent diffusion have been used in one and two dimensions to study the flame structure and burning rate behavior.
- One example is the work of Miller and Anderson (2000) who have developed detailed models to study flame structure and predict burning rates of multi-ingredient DB propellants

Comparison of calculated burning rate of a JA2 propellant with measured data

JA2 propellant example:
60% by wt NC
15% by wt NG
25% by wt DEGDN

Mole fractions of Condensed-Phase Decomposition Products at Propellant Surface:

NO2	0.2771
HONO	0.0579
CHOCHO	0.0211
HCO	0.1050
CH2O	0.2415
CH2	0.0919
CH3	0.0140
CH4	0.0070
CO	0.1574
H	0.0271

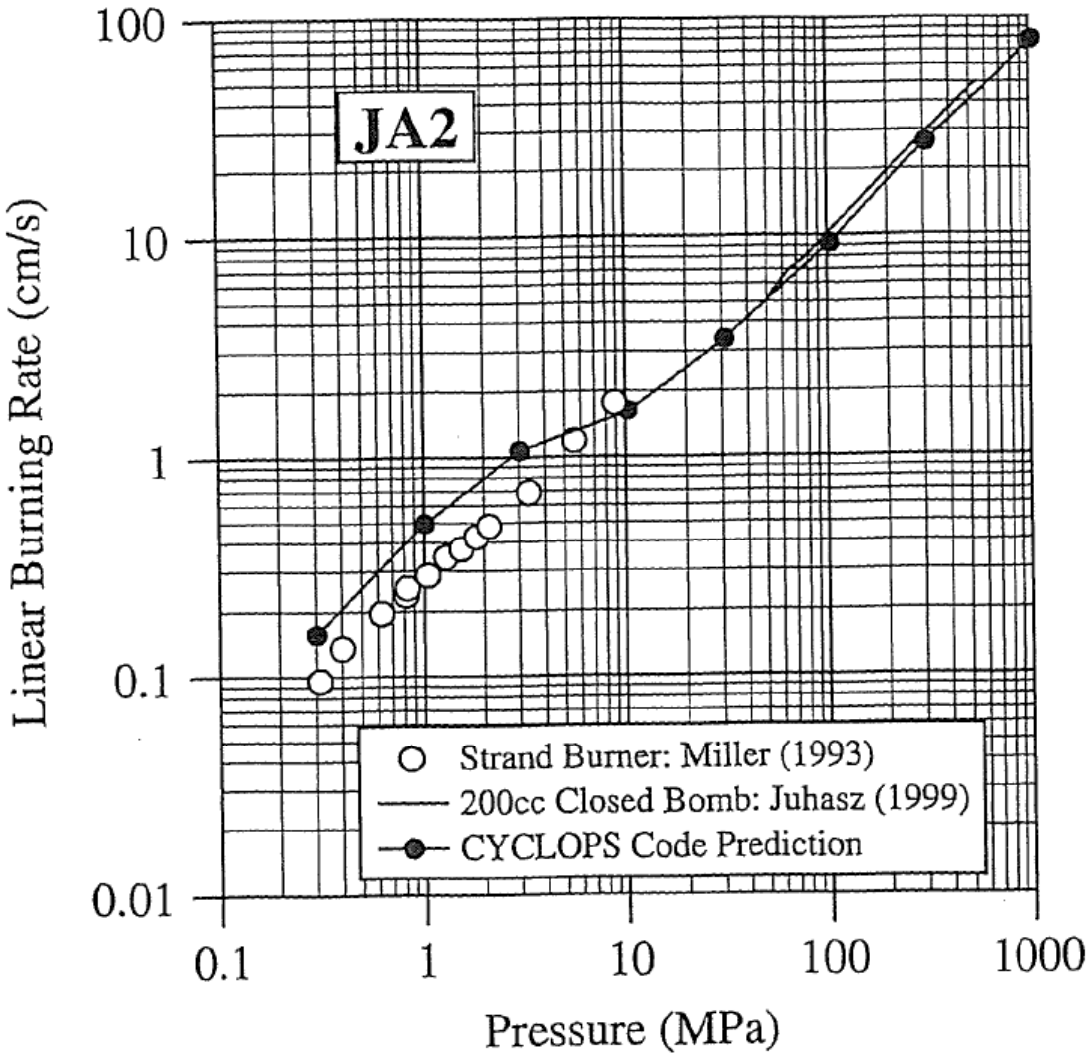

Miller and Anderson (2000)

Comparison of measured and calculated temperature and NO mole fraction profiles for a JA2 propellant at T_i = 294 K

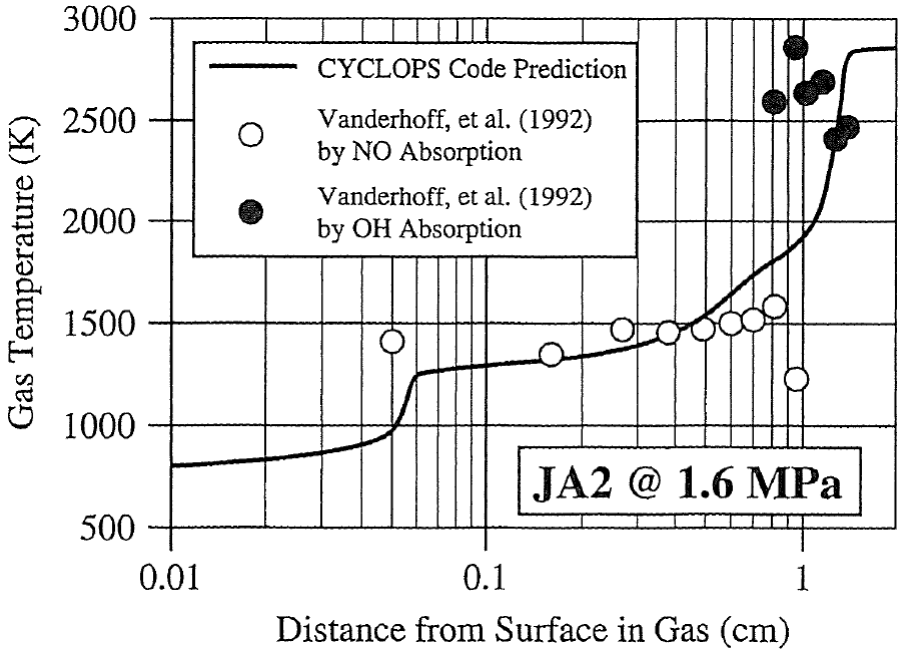

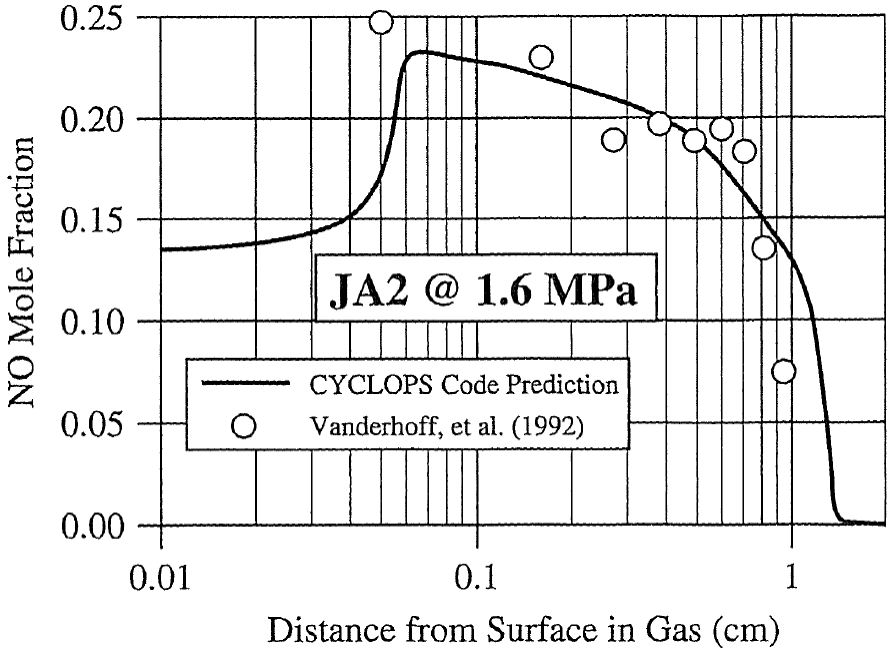

Miller and Anderson (2000)

Thermal Decomposition Mechanisms of RDX

- *Homolytic cleavage of an N-N bond* to form NO_2 plus a residual molecule RDR $(H_2CNNO_2)_2(H_2CN)$, which subsequently decomposes to form various products
- *Concerted decomposition of the ring* to form three methylene nitramine molecules (MN; H_2CNNO_2)
- *Successive HONO elimination* to form three HONO and 1,3,5 triazine (TAZ, $C_3H_3N_3$), with subsequent decomposition to three HCN molecules

Decomposition of RDX at High Temperatures

C.F. Melius, "Thermochemical Modeling: I. Application to Decomposition of Energetic Materials," and "Thermochemical Modeling: II. Application to Ignition and Combustion of Energetic Materials," Chemistry and Physics of Energetic Materials, 21-78, S.N. Bulusu (ed.), Kluwer Academic Pub.

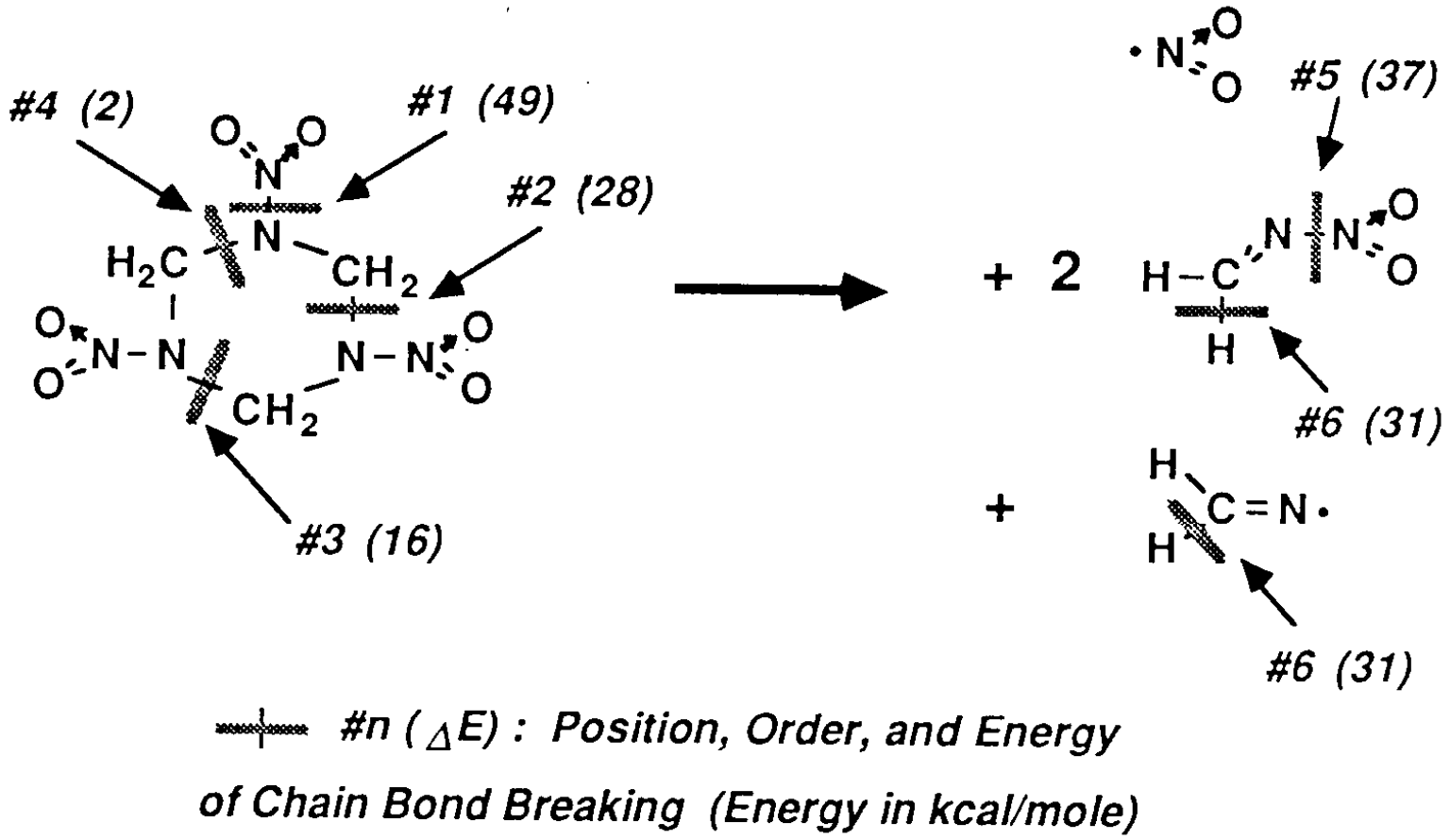

Potential Energy Profile for RDX Thermal Decomposition via Homolytic N-NO_2 Bond Cleavage

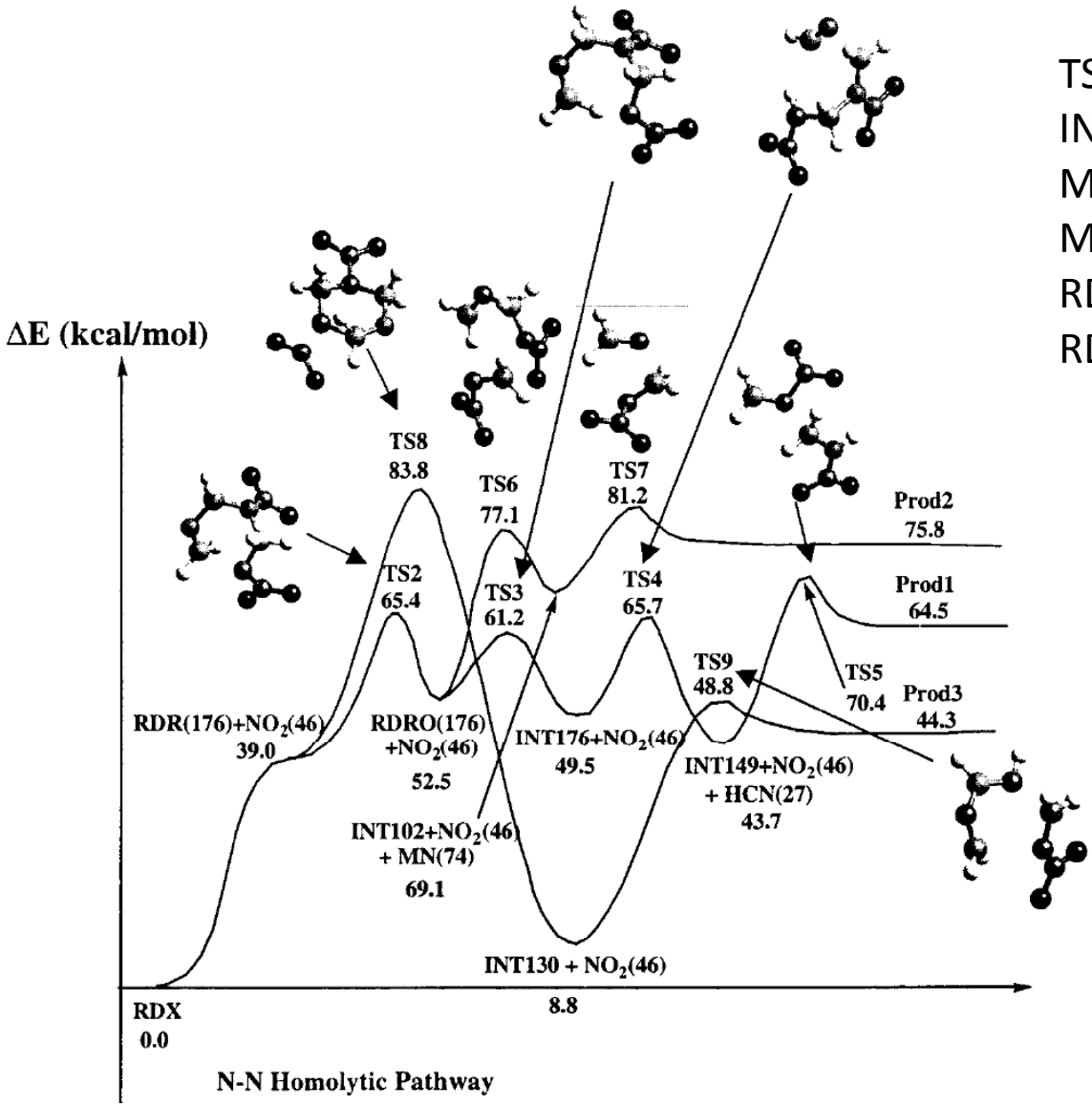

TS – Transition State
INT – Intermediate Species
MN – Methylene nitramine (CH_2NNO_2)
MNH - $CH_2NHCHNNO_2$ radical
RDR – RDX after losing one NO_2
RDRO – RDR with the C-N ring opened

Prod1: RDX$\rightarrow NO_2$+HCN+MN+MNH + ΔH_{r1} (=64.5 kcal/mol)

Prod2: RDX$\rightarrow NO_2$+2MN+CH_2N+ ΔH_{r2} (=75.8 kcal/mol)

Prod3: RDX$\rightarrow 2NO_2$+MN+CH_2NCHNH+ ΔH_{r3}(=44.3 kcal/mol)

From Chakraborty et al., 2000)

Potential Energy Profile for RDX Thermal Decomposition via HONO Elimination

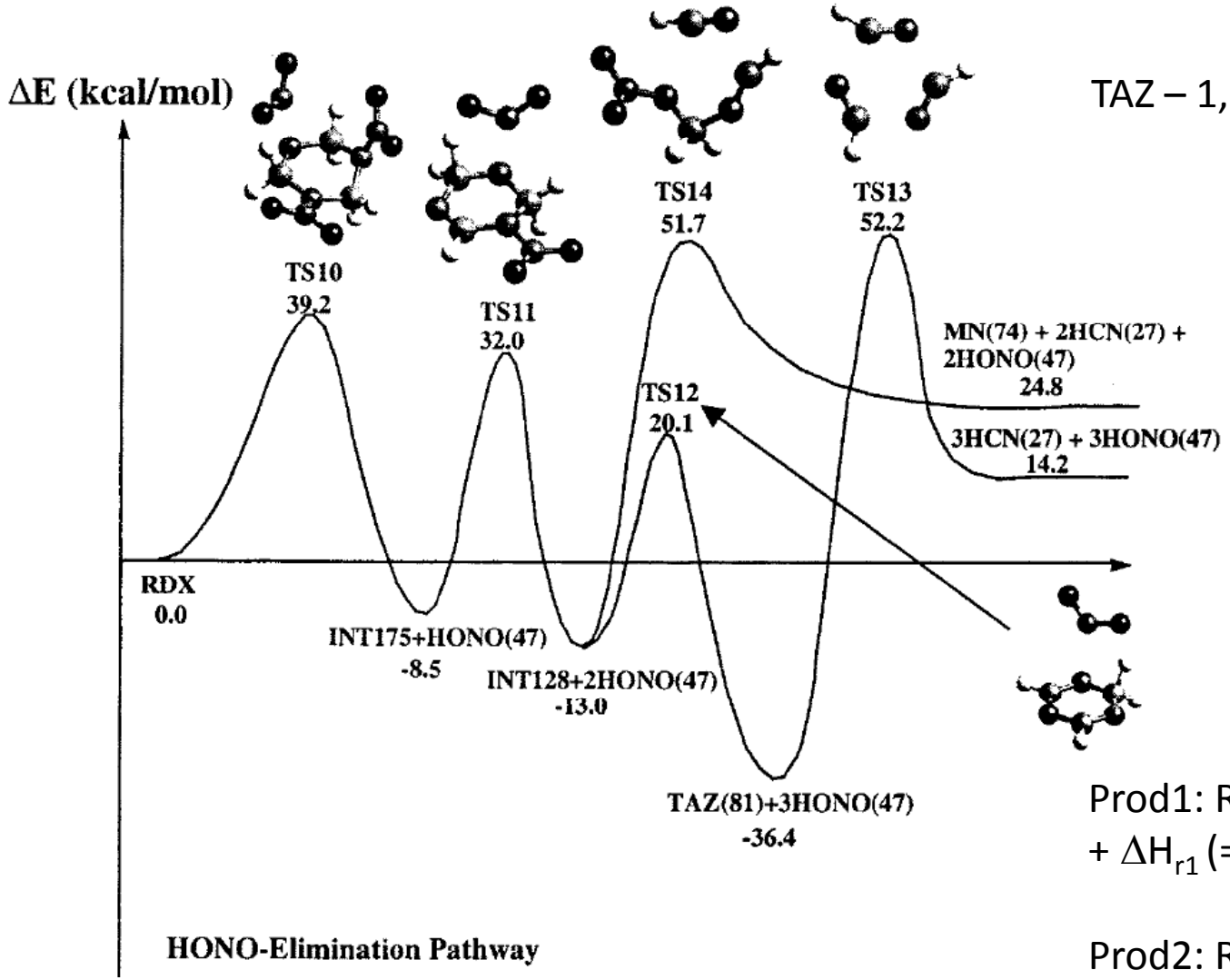

TAZ – 1,3,5 triazine $C_3H_3N_3$

Prod1: RDX→2HONO+MN+2HCN + ΔH_{r1} (=24.8 kcal/mol)

Prod2: RDX→3HONO+3HCN+ ΔH_{r2} (=14.2 kcal/mol)

From Chakraborty et al., 2000)

Condensed Phase Chemical Kinetic Studies

Experiment	Heating Rate
Simultaneous thermogravimetric modulated beam mass spectroscopy (STMBS) R. Behrens - Sandia	10^{-2} K/s
T-jump/FTIR T. Brill - U Delaware Confined Rapid Thermolysis S. Thynell – Penn State	10^{3} K/s
Pulsed laser heating / thermal quench C. Wight - U Utah	10^{7} K/s

Measured N_2O/NO_2 ratio after 10 s at 5 atm Ar from T-jump/FTIR spectroscopy of HMX and RDX

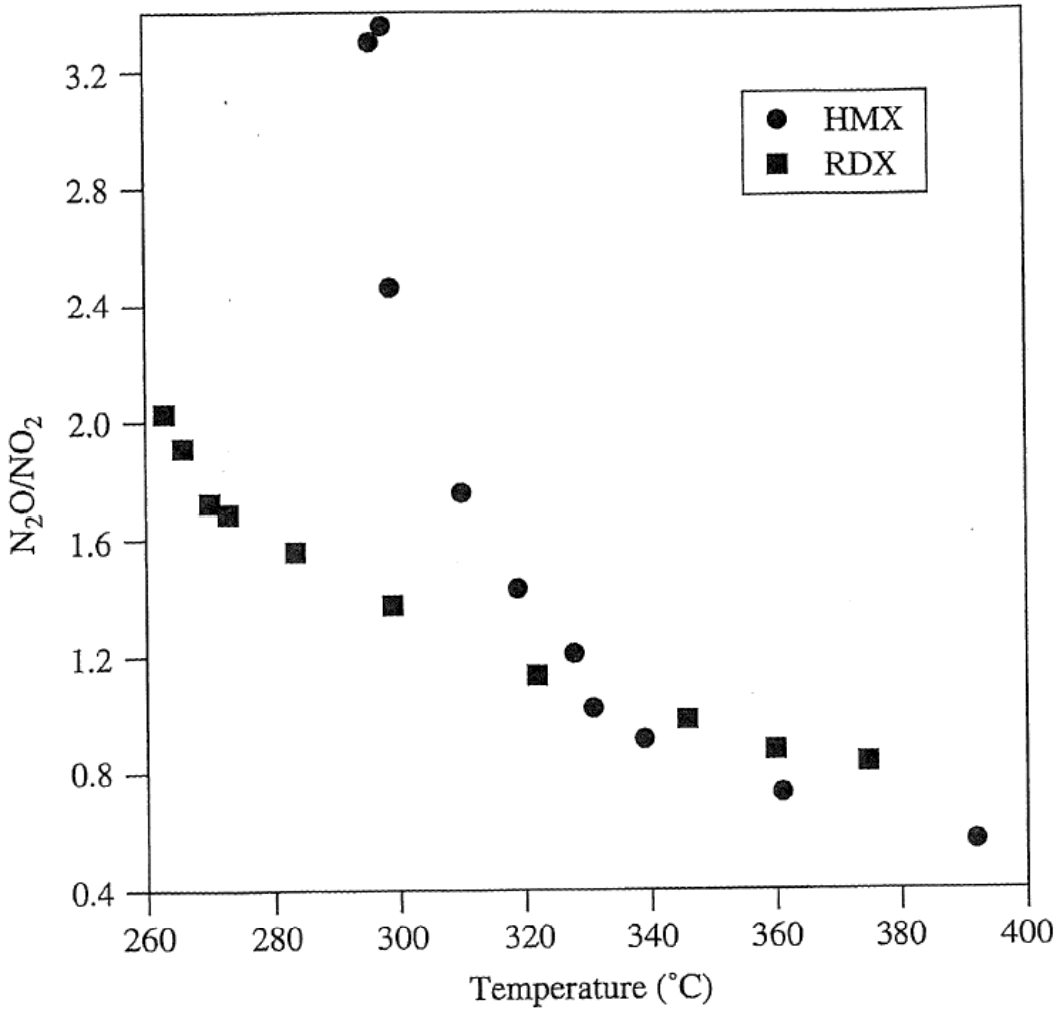

after Brill, 1995

Condensed-Phase Reaction Mechanisms

T.B. Brill, J. Prop. Power, 11, 4, 1995; S. Thynell, P. Gongwer, and T.Brill,J. Prop. Power, 12, 933, 1996

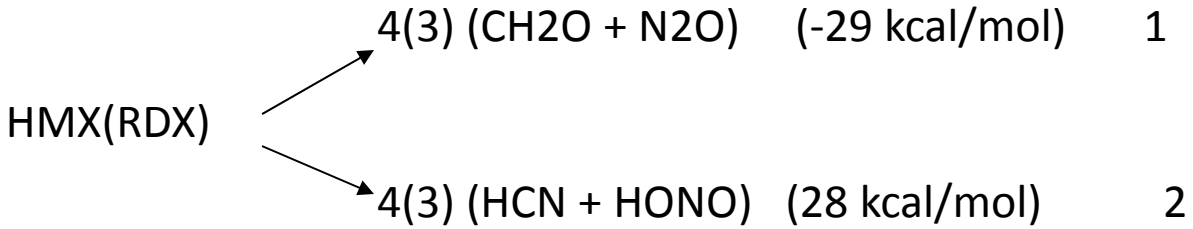

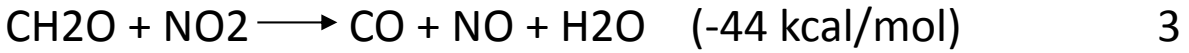

RDX Thermal Decomposition Rate Parameters

Reaction	1	2	3
A	$6x10^{13}$ s^{-1}	$16x10^{16}$ s^{-1}	$802x\ T^{2.77}$ cm^3/mol-s
E	36 kcal/mol	45 kcal/mol	25.73 kcal/mol

E.S. Kim and S.T. Thynell, "Condensed Phase Rates of RDX from Confined Rapid Thermolysis/FTIR Spectroscopy," AIAA 98-3828, 34th AIAA Propulsion Conference and Exhibit, Cleveland, OH, July 13-15, 1998

Global 10 step condensed phase reaction mechanism obtained by inverse-based iterative fitting

Thermal Decomposition of Liquid Phase RDX

- Elementary reactions identified using *ab initio* quantum chemistry methods including density functional theory
- Liquid phase reactions are simulated using the conductor-like polarizable continuum for solvation with water as solvent

P1: HONO elimination

P2: N-NO_2 homolysis

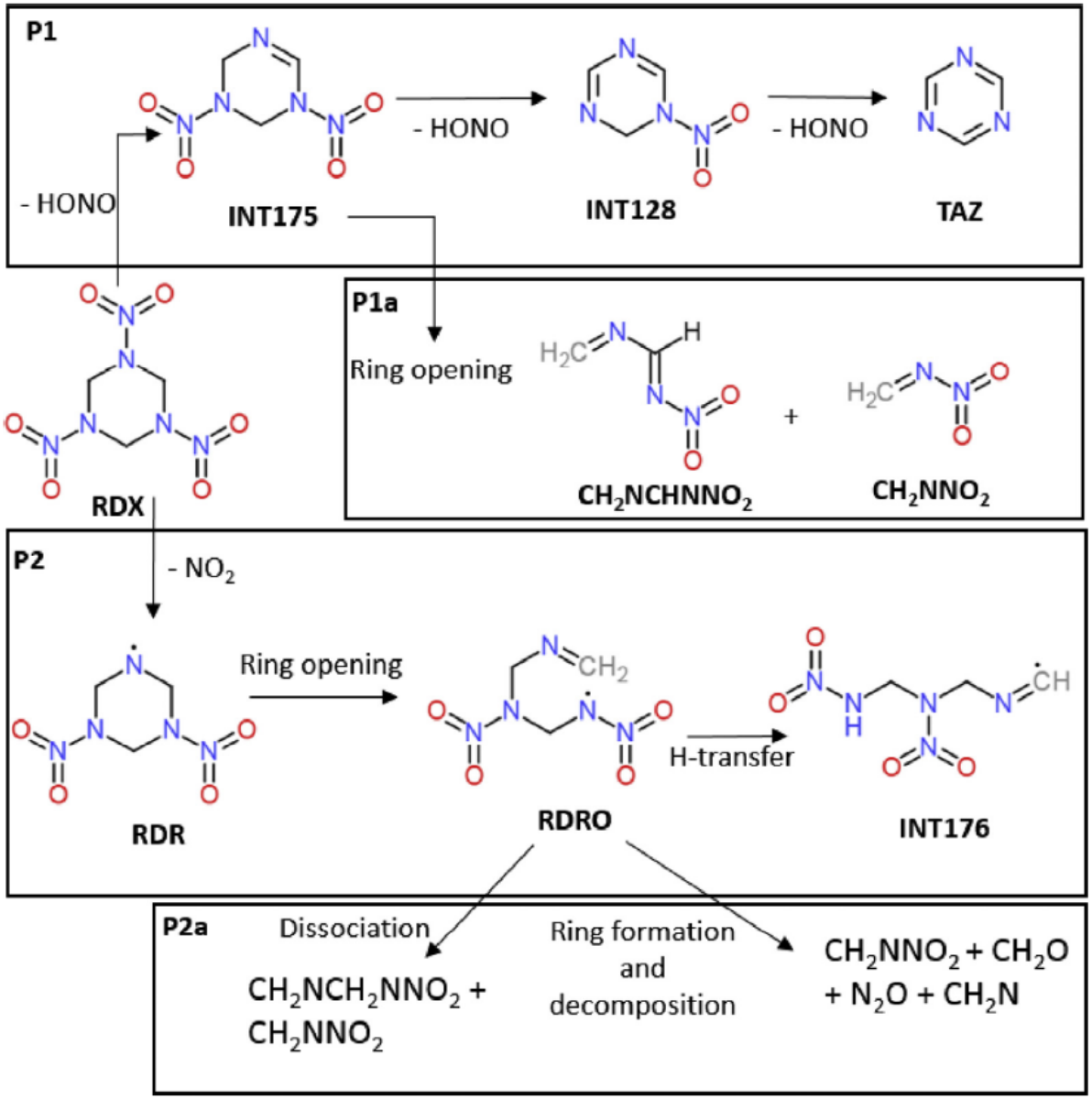

Patidar and Thynell, Combustion & Flame, Vol. 178, April 2017

Thermal Decomposition of Liquid Phase RDX

P3: Reaction with NO and formation of ONDNTA

P4: Prompt oxidation via HONO and $ONNO_2$ addition

P5: Hydrogen abstraction via NO_2

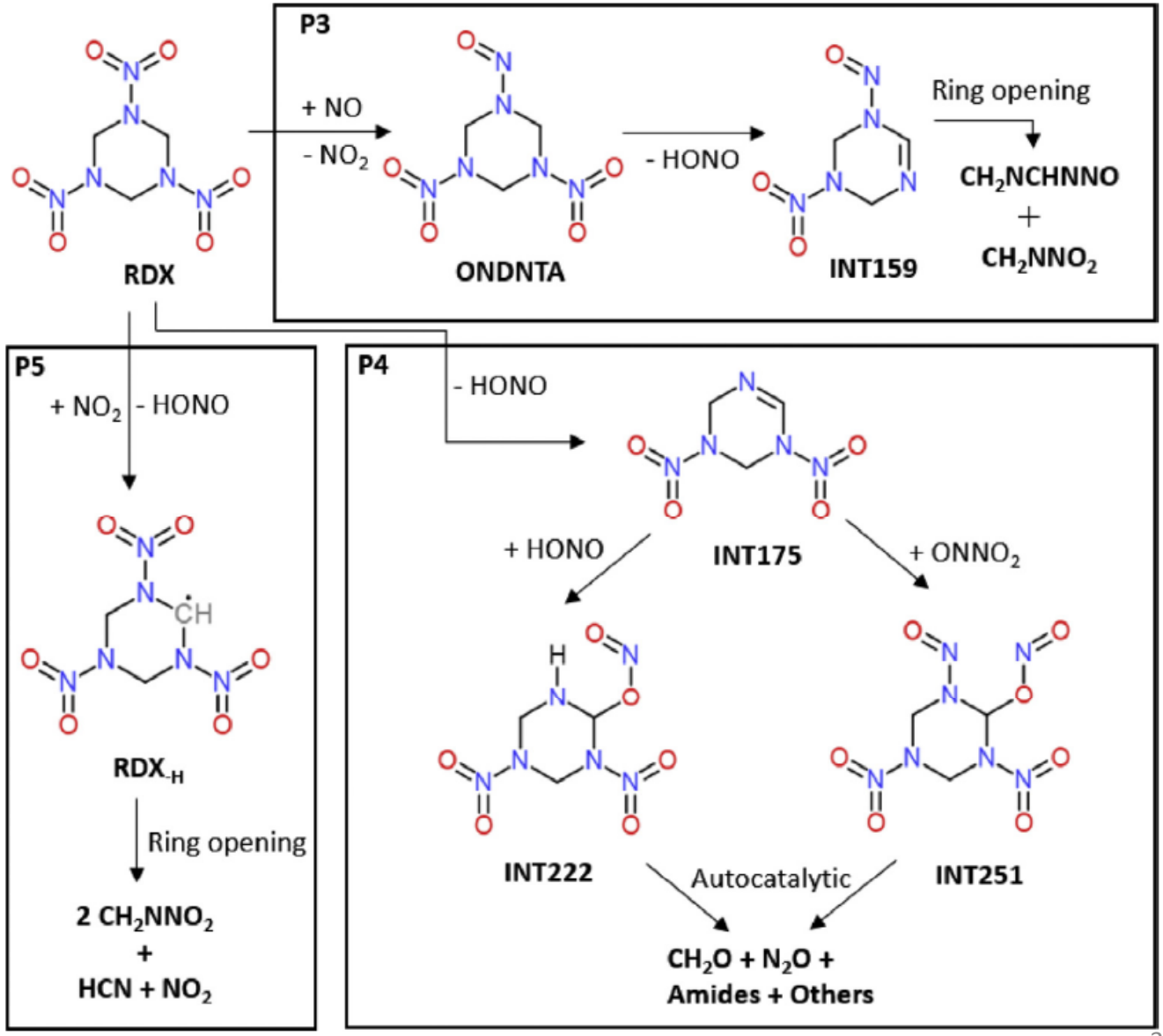

Patidar and Thynell, Combustion & Flame, Vol. 178, April 2017

Thermal Decomposition of Liquid Phase RDX

- Confined rapid thermolysis/FTIR spectroscopy, where 0.5mg of RDX is heated at 2000K/s to 548 K at 1 atm
- HONO elimination is more significant than N-NO_2 homolytic cleavage in liquid phase
- HONO elimination is followed by ring opening instead of successive HONO elimination

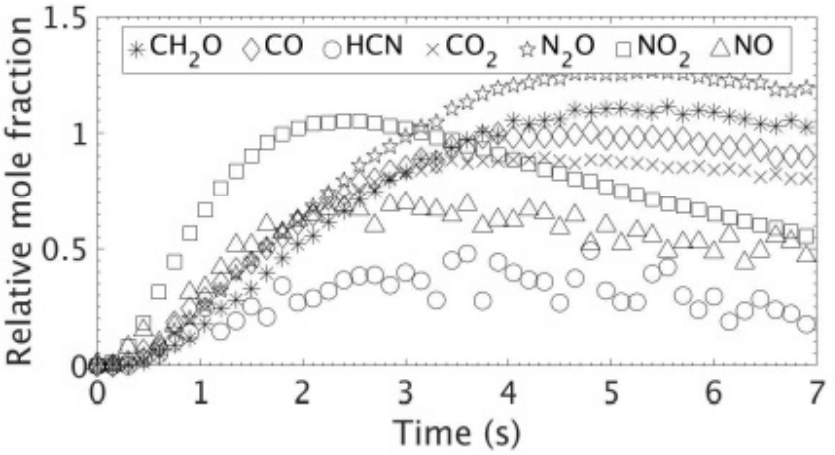

experiment

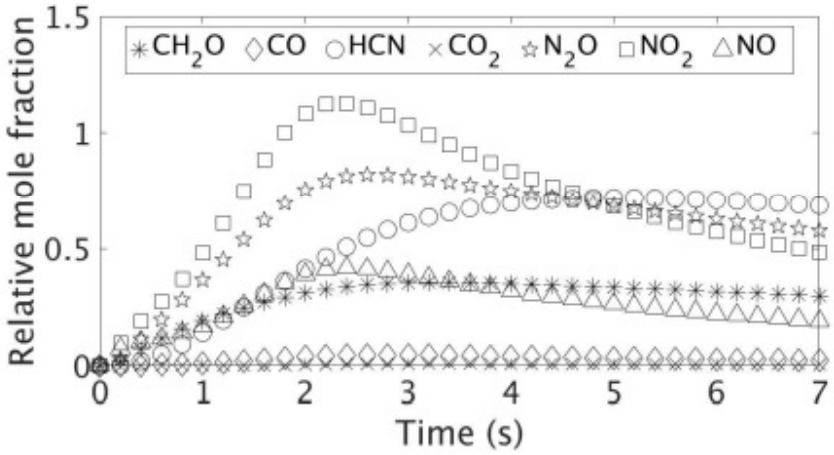

model

From Patidar and Thynell, Combustion & Flame, Vol. 178, April 2017, pp. 7–20; Khichar, Patidar and Thynell, 10th National Combustion Meeting, April 23-26, 2017; results on HMX decomposition is also presented at the 10th National Combustion Meeting.

Temperature Profiles in Various Flame Zones and Condensed-Phase Regions of Nitramine Monopropellant

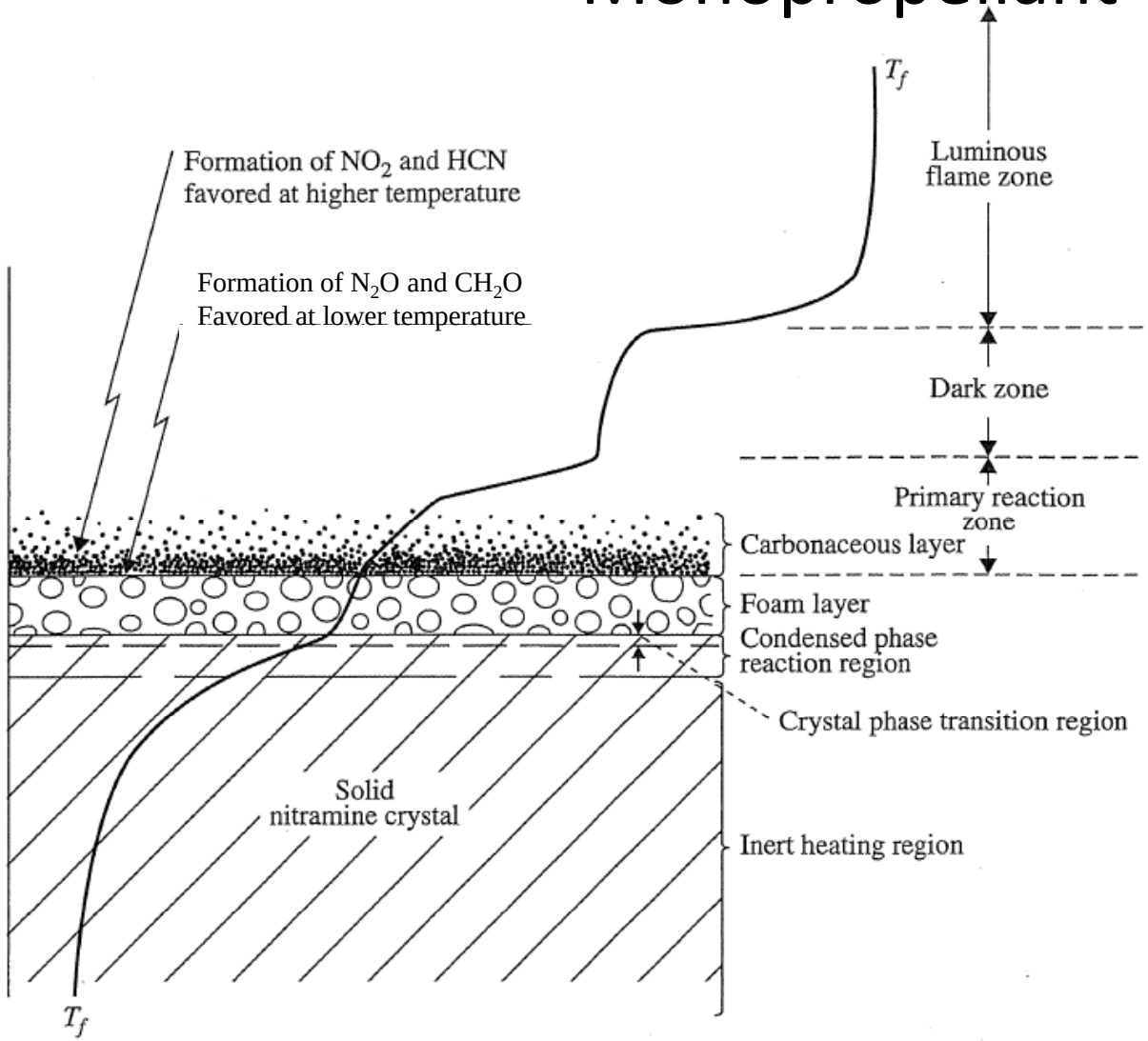

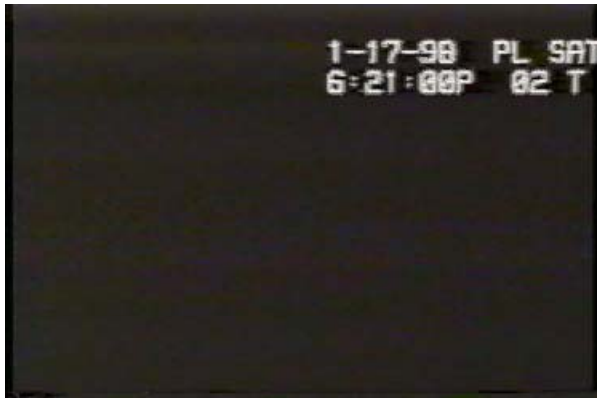

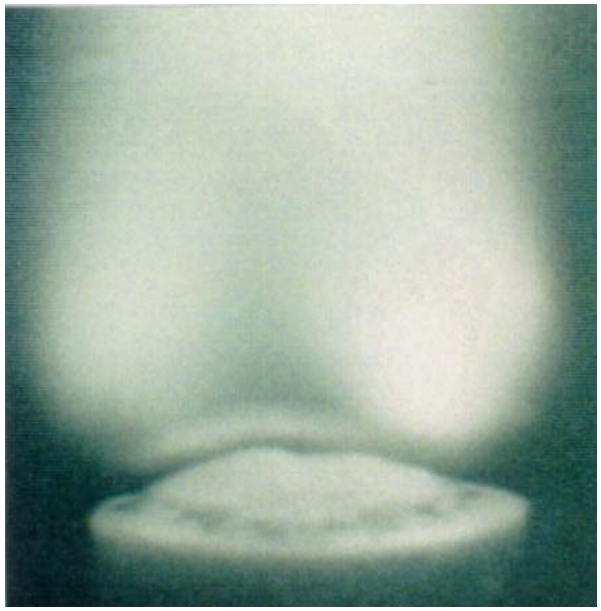

RDX

Modeling of RDX Combustion

- Numerical models have included detailed chemical kinetics and transport phenomena in the gas-phase and thermal decomposition and subsequent reactions in the condensed phase
- Formation of gas bubbles in the subsurface layer to molecular degradation and evaporation has also been included
- Model for RDX Combustion by Liau and Yang

RDX Monopropellant Deflagration Effect of Pressure

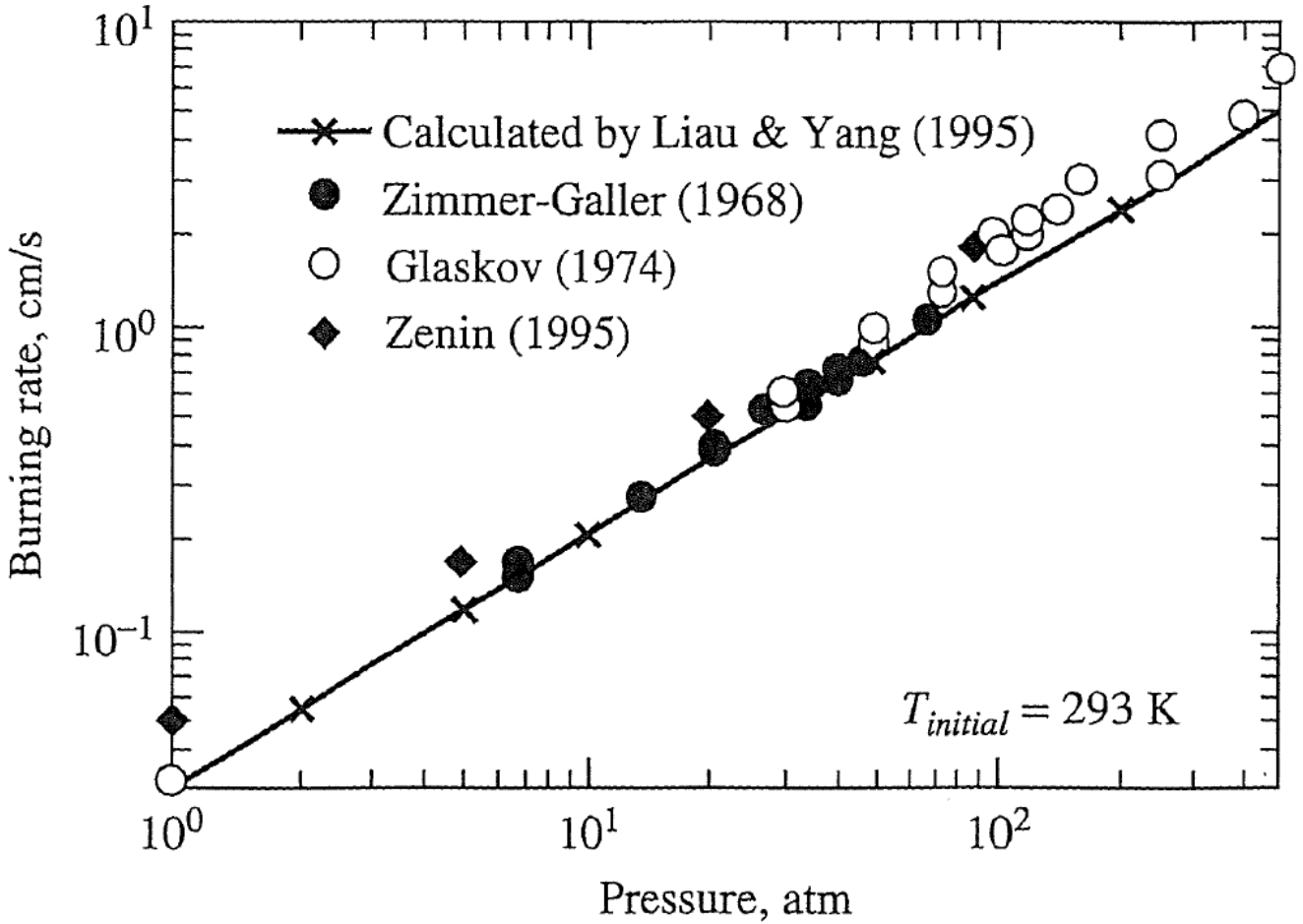

Calculated temperature Profiles of Self-Sustained RDX Combustion at Various Pressures

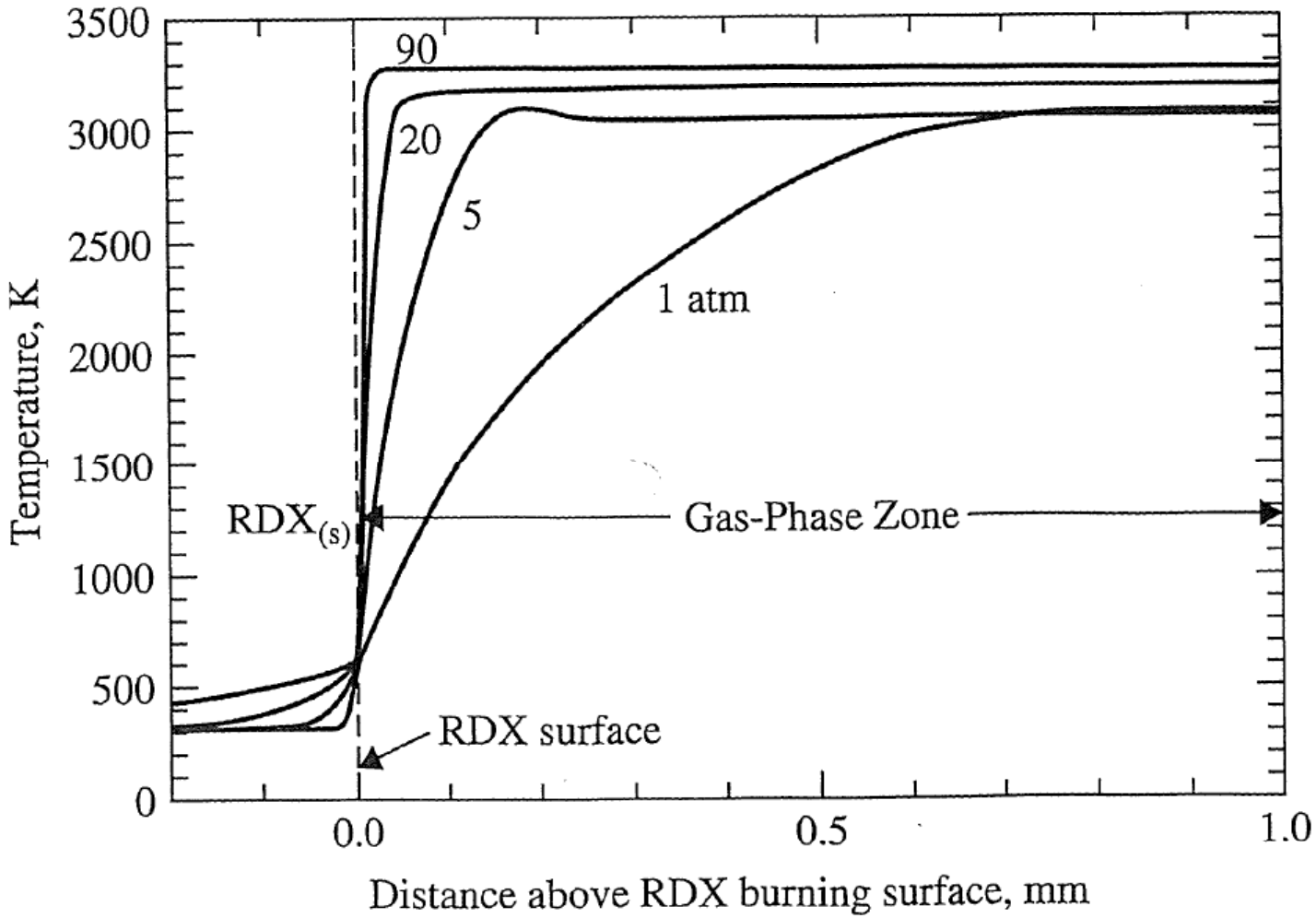

Comparisons of Calculated and Measured Major Species Concentrations at P=0.5 atm

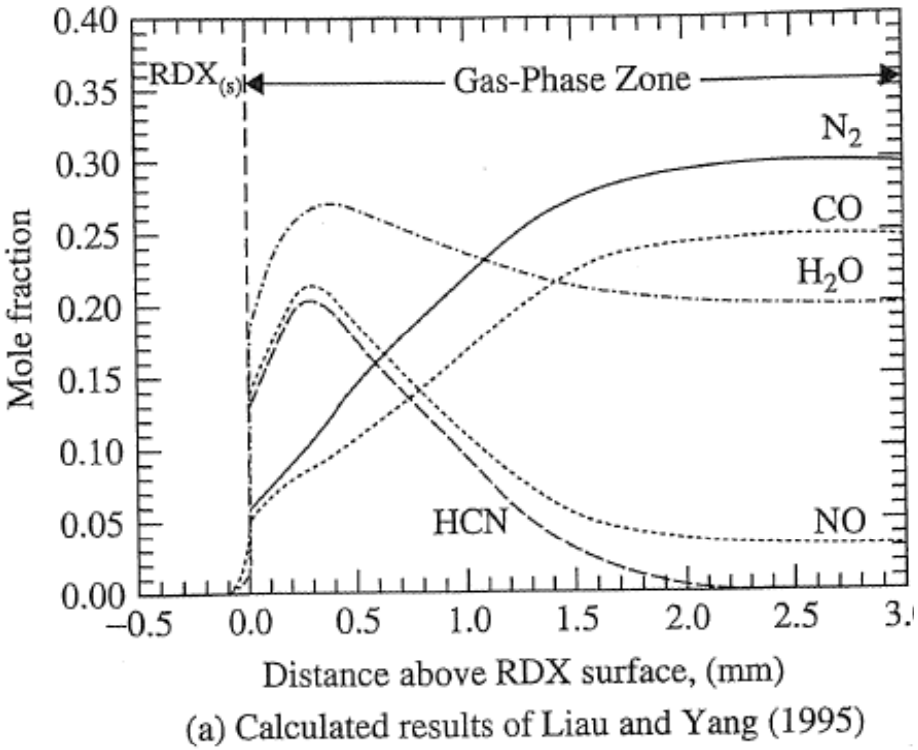

(a) Calculated results of Liau and Yang (1995)

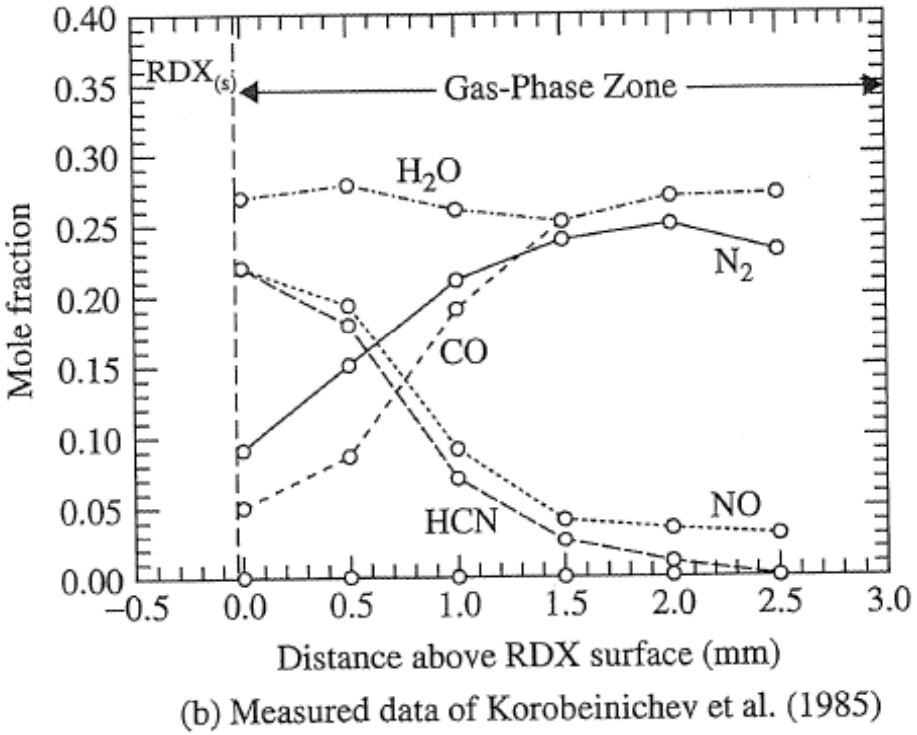

(b) Measured data of Korobeinichev et al. (1985)

Effect of Pressure on Foam Layer Thickness, Surface Temperature, and Void Fraction for RDX Deflagration

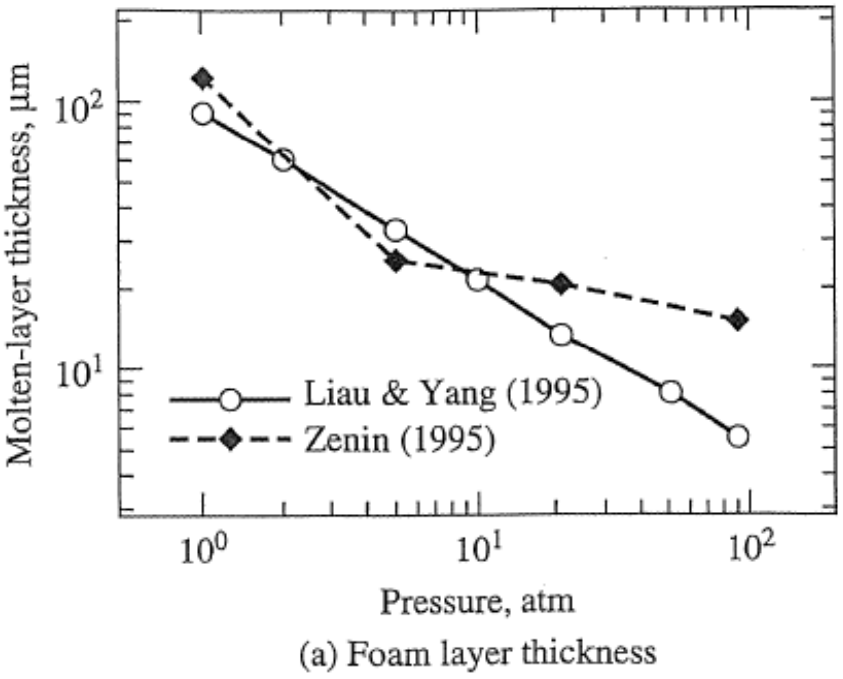

(a) Foam layer thickness

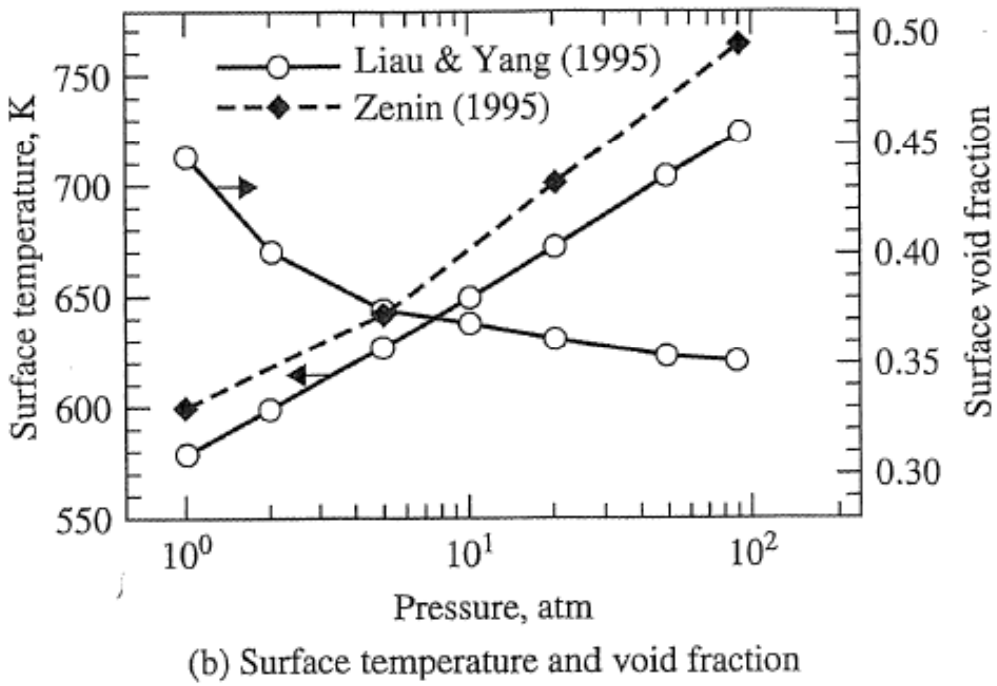

(b) Surface temperature and void fraction

Temperature Sensitivity Calculations

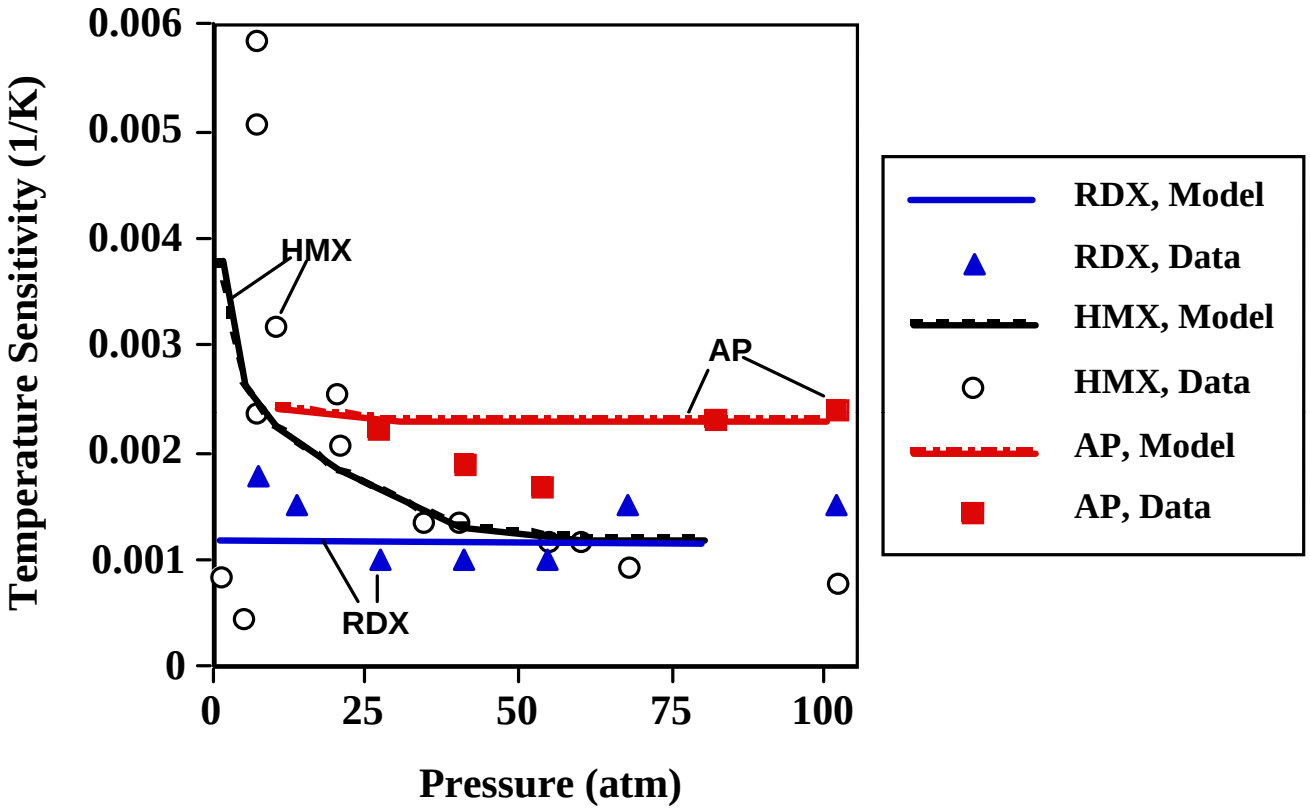

- HMX σ_p increases dramatically at low pressure
- RDX σ_p increases slightly at low pressure
- AP σ_p ~constant
- Washburn HMX condensed phase model includes Marangoni surface tension effect

Washburn & Beckstead 2006

Typical Solid Composite Propellant Mixture

~12% Binder (HTPB)
~18% Aluminum
~70% Oxidizer

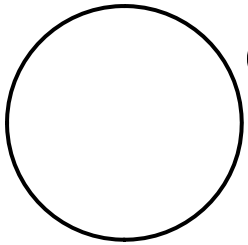

Fine oxidizer ~1-15 μm (bacteria to talcum powder)

Aluminum ~ 20-50 μm

Medium oxidizer ~ 20-90 μm (white blood cell to hair)

Coarse oxidizer ~ 200-400 μm (fine to medium beach sand)

- Very heterogeneous burning surface
- Dimensions don't allow direct combustion measurements
- Crystals are not round - irregular shapes

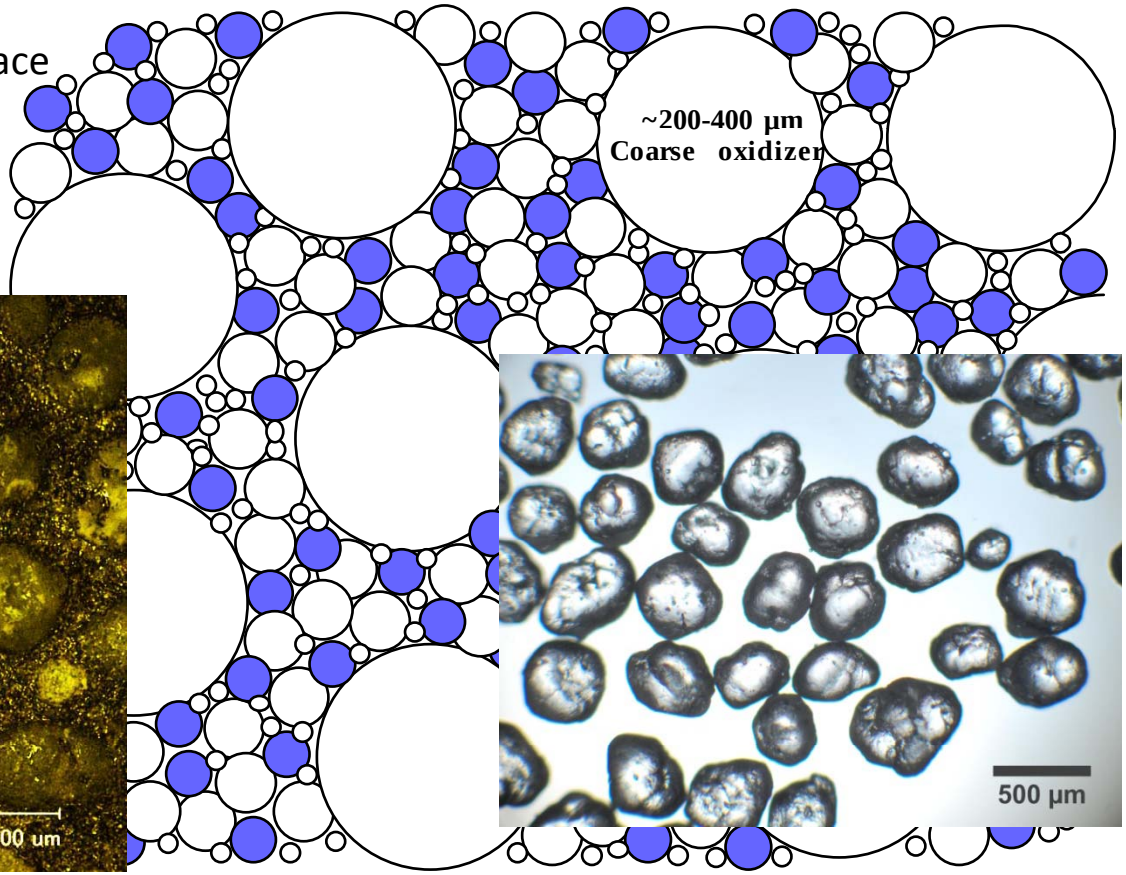

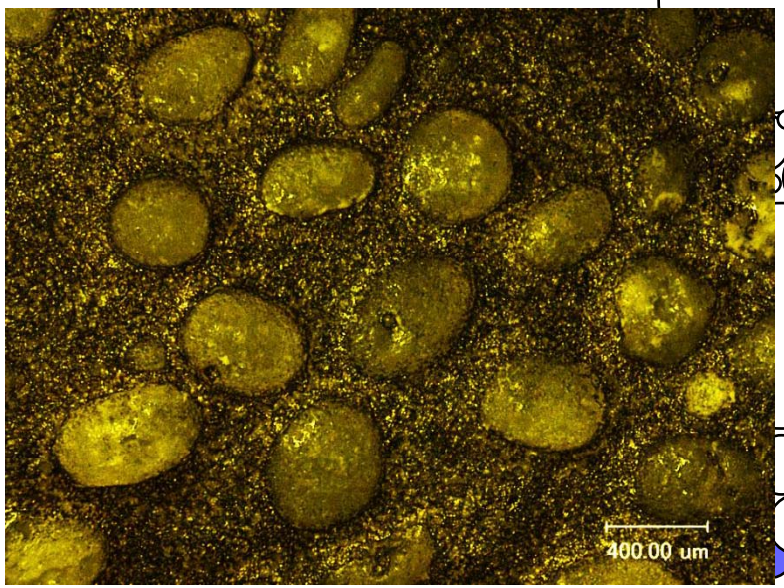

Hierarchical Approach Applied

Start with the simplest systems and work up, with validations at each step

- 1-D Monopropellant: Single ingredient
  - –Gas phase and condensed phase chemistry development
  - –Surface regression models
- 1-D Composite propellant: Add chemical complexity without spatial complexity
  - –Chemistry interaction
- 1-D Counterflow: Add diffusion flame, but remain 1-D
  - –Chemistry with fluid dynamics
  - –Oxidizer with binder decomposition product chemistry

Hierarchical Approach – cont'd

- 2-D Sandwich and axisymmetric: Idealized diffusion flame in 2-D
  - Multidimensional flames
  - Full fluid dynamic coupling
  - Surface regression interactions
- 2-D with realistic packing: Diffusion flame interactions and evolving surface geometry
  - Simulation of oxidizer/binder distribution
  - Platform for development of reduced chemical models
- 3-D with realistic packing: Full propellant system
  - Propellant design tool

Why Kinetics Based Models Necessary

- I_{SP} and T_f easily calculated from thermodynamics, but...
- *Kinetics* controls *critical* ballistic properties
  - Burning rate, pressure exponent, T sensitivity, ignition and transient combustion, combustion instability, cookoff, DDT
- *Must* know ballistics to design rocket motor
  - *Only 33% error in burning rate can lead to 300% overpressure and catastrophic failure of system*
  - *Pressure exponent critical to system design, for example...*
    - Mesa for operational stability or high exponent for pintle throttlability
- Global Models Inadequate
  - Don't uncover real kinetic mechanism
  - Can't predict combustion instability, ignition, DDT etc.
  - Can't help design new propellants based on new materials

AP Propellant Properties

- AP is very atypical oxidizer
- Widely used oxidizer
- Significantly increased burning rates relative to pure AP
- Significant particle size effect
  - Smaller particles → faster rate
- 30% excess O_2
- 1.3 hazard classification
  - PDL ~ 20 atm
  - ΔH_f -71 kcal/mol
- Chlorine chemistry
  - HCl products

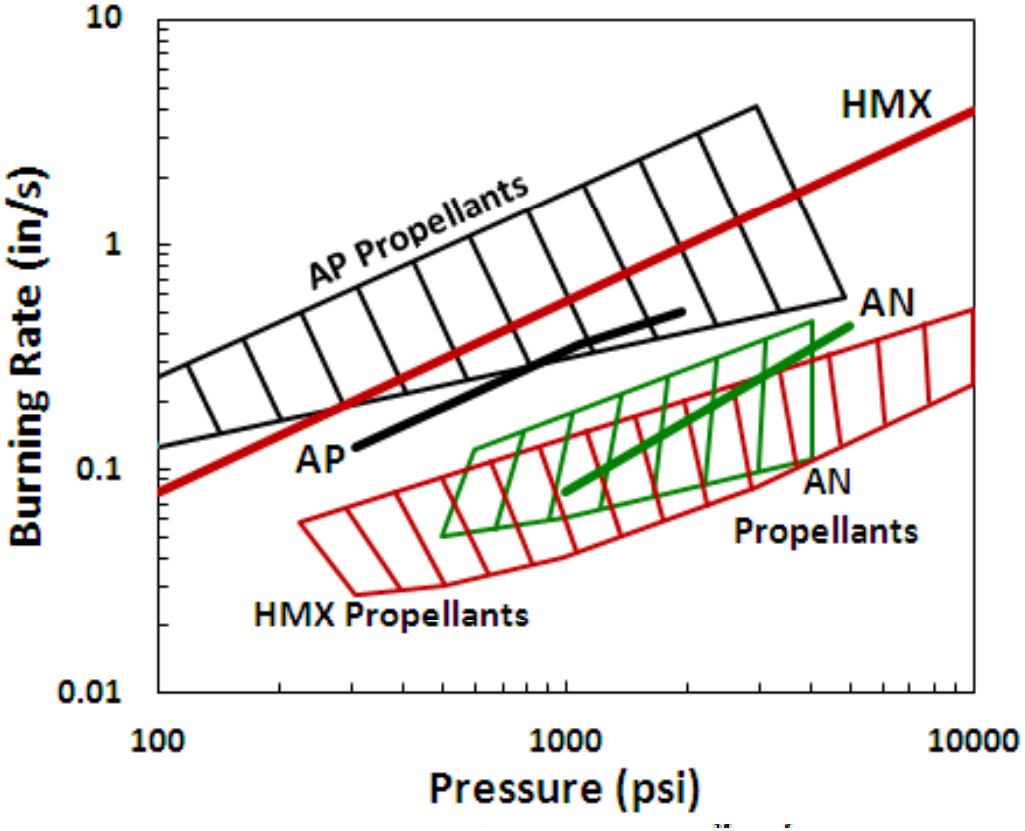

Beckstead, M.W., 26th JANNAF CS, (1989)

Composite AP-based solid propellants use a bimodal distribution of particle sizes for increasing propellant density and controlling burning rate

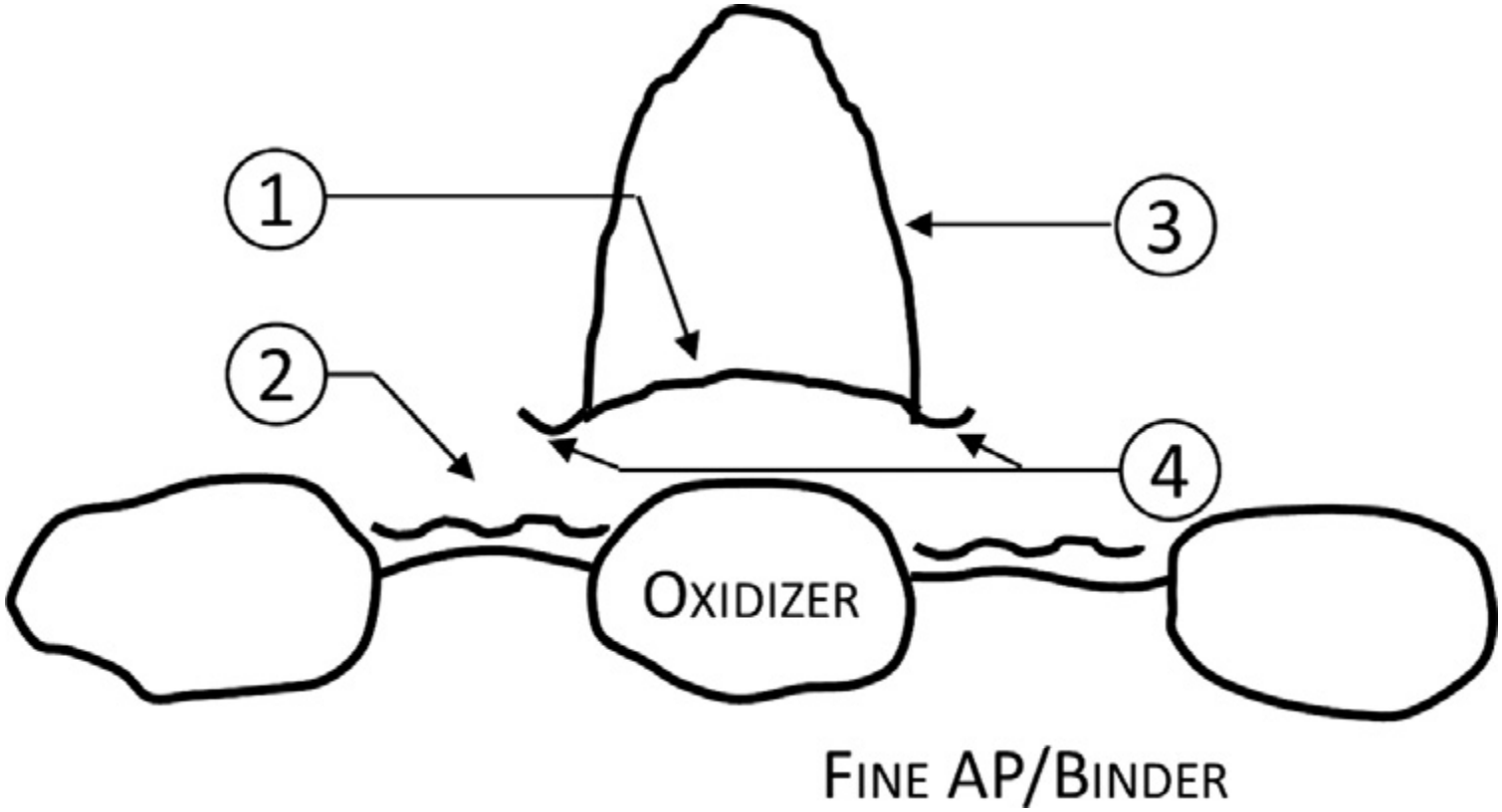

Microscale flame structure above a bimodal composite AP propellant. Represented here are the (1) monopropellant flame, (2) pseudo-premixed flame, (3) final diffusion flame, and (4) leading-edge flame.

From M.L. Gross and M.W. Beckstead, J. Propulsion Power 25 (2009) 74-82

AP Decomposition Kinetics and Monopropellant Deflagration

- Chen and McQuaid (2014 JANNAF CS Meeting) have developed the most recent gas-phase mechanism consisting of 788 reaction rate expressions and 105 species
- The condensed phase mechanism remains uncertain. Most recently, Zhu and Lin (J. Phys. Chem. C 112 (2008) 14481) proposed a dissociative sublimation mechanism of crystal NH_4ClO_4(c) that involves a NH_3…$HClO_4$(g) complex

  $NH_4ClO_{4(}c)\leftrightarrow NH_4ClO_4(s) \leftrightarrow NH_3…HClO_4(g) \leftrightarrow NH_3(g)+HClO_4(g)$

  where NH_4ClO_4(s) corresponds to a relaxed surface of the crystal

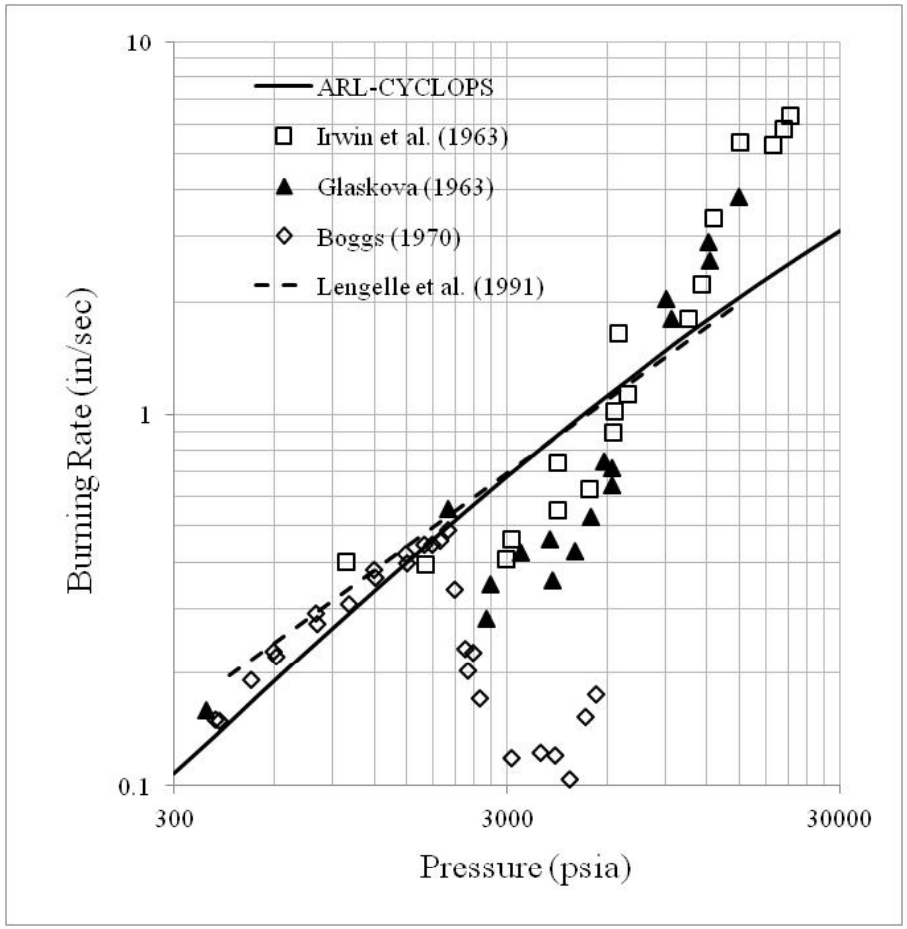

Chen and McQuaid (2014 JANNAF CS Meeting

Propellant Surface and Sub-Surface

- Condensed phase and interface/surface phenomena is the least understood
  - The surface reaction zone is very thin, multiphase, and has a steep temperature gradient
- Several studies used cinephotomicrography to observe burning surface, then sample was quenched and examined using scanning electron microscopy
- Other studies used fast thermolysis and FTIR to measure decomposition products
- Typically microthermocouples are embedded within propellant sample at various distances from the surface to measure thermal response of propellant
- Need information on condensed phase reactions, AP phase changes and binder decomposition before reaching the burning surface

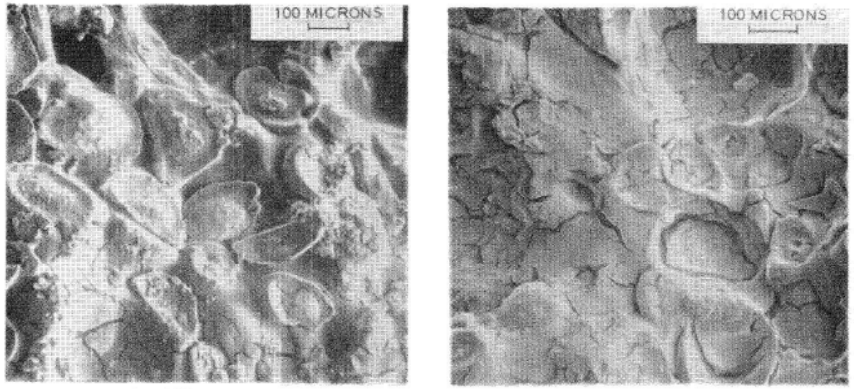

A. 100 PSIA (102×) B. 800 PSIA (120×)

R. Derr and T. Boggs, Combustion Science and Technology, 1:5, 369-384, 1970.

1-D Diffusion Flame

- 1D counter-flow configuration
  - Oxidizer + binder chemical interaction without spatial complexity
  - 1D flame allows rapid turn around 1D model
  - Enormous expansion of length scale
    - Sandwich flame standoff 100 microns
    - Counter-flow standoff 5 mm

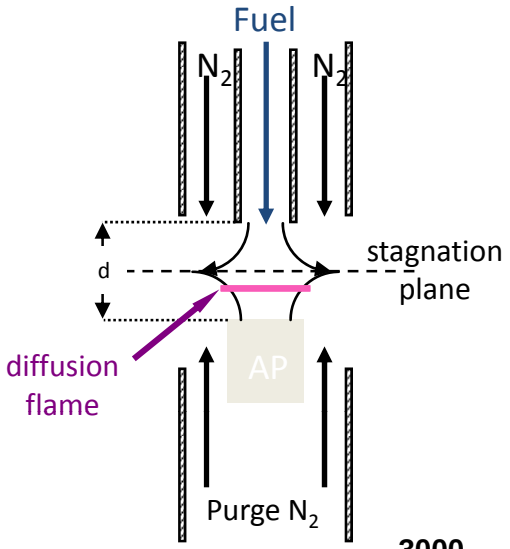

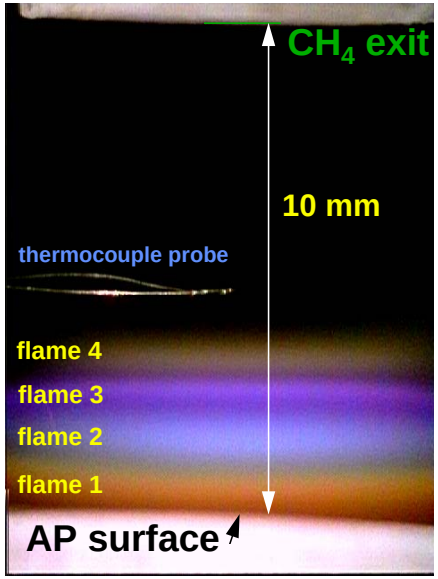

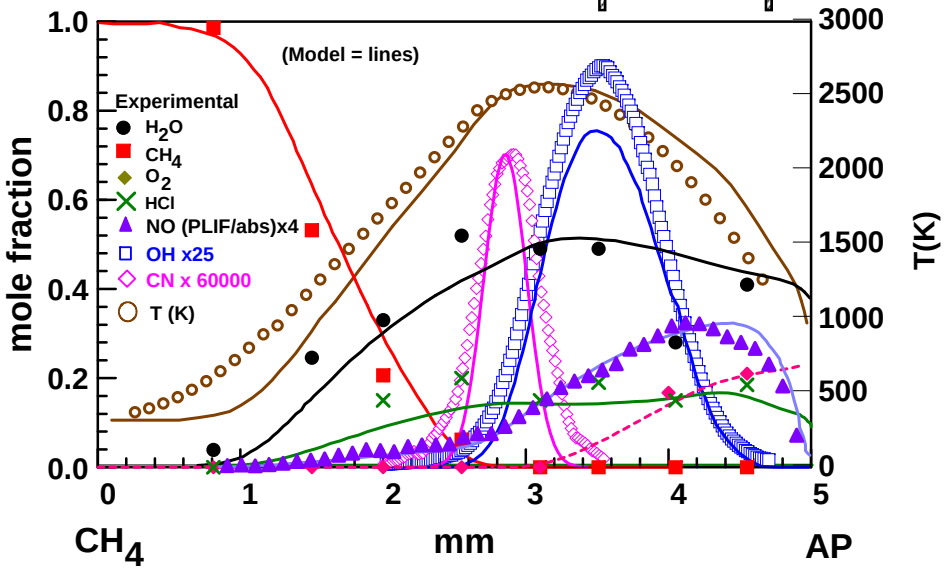

From M.D. Smooke, R.A. Yetter, T.P. Parr, D.M. Hanson-Parr, Proc. Combust. Inst. 28 (2000) 839–846. T.P. Parr, D.M. Hanson-Parr, M.D. Smooke, R.A. Yetter, Proc. Combust. Inst. 29 (2002) 2881–2888. T.P. Parr, D.M. Hanson-Parr, M.D. Smooke, R.A. Yetter, Proc. Combust. Inst. 30 (2005) 2113–2121.

2D Gaseous Fuel AP Diffusion Flames

- With kinetics finalized via 1D counter-flow flames, extended model and experiment to 2D geometry
- Started with simplicity of the same gaseous fuel (methane or ethylene) as 1D work
- Axisymmetric (experiment and modeling)
  - Small fuel hole in center of big domain of AP Drilled hole in AP pellet
  - 990 μm down to 60 μm
  - O-ring seal to AP cylinder
  - CH_4 fed below at desired rate
  - CH_4 exit velocity was 9.75 m/sec peak, parabolic flow

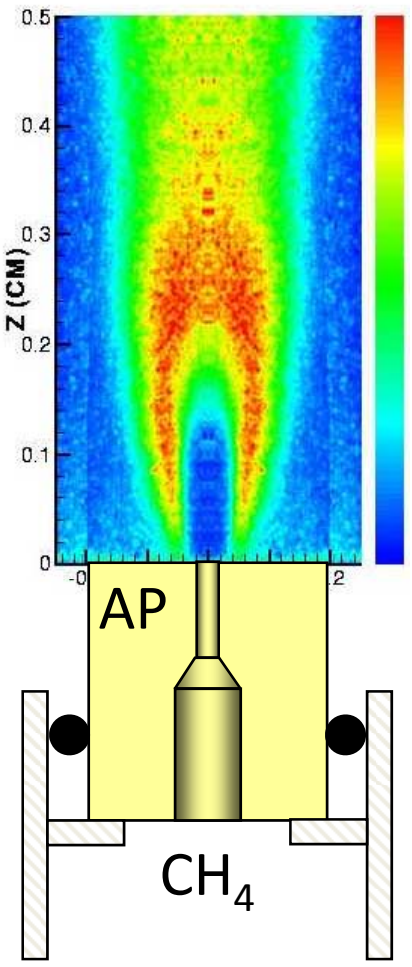

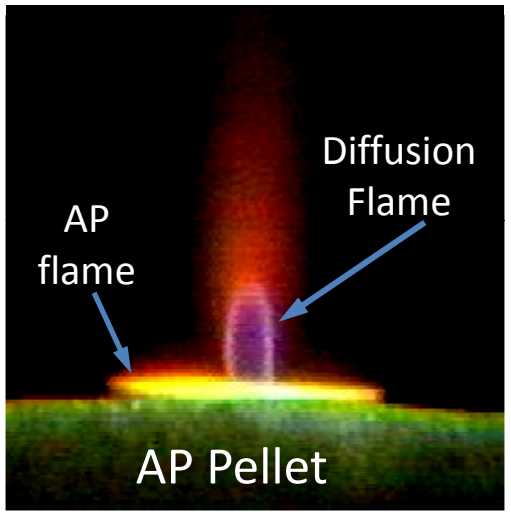

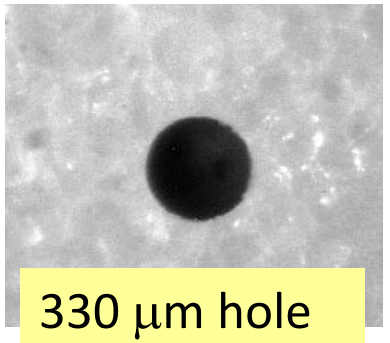

From M.D. Smooke, R.A. Yetter, T.P. Parr, D.M. Hanson-Parr, Proc. Combust. Inst. 28 (2000) 839–846. T.P. Parr, D.M. Hanson-Parr, M.D. Smooke, R.A. Yetter, Proc. Combust. Inst. 29 (2002) 2881–2888. T.P. Parr, D.M. Hanson-Parr, M.D. Smooke, R.A. Yetter, Proc. Combust. Inst. 30 (2005) 2113–2121.

Effects of pressure and particle size on burning rate

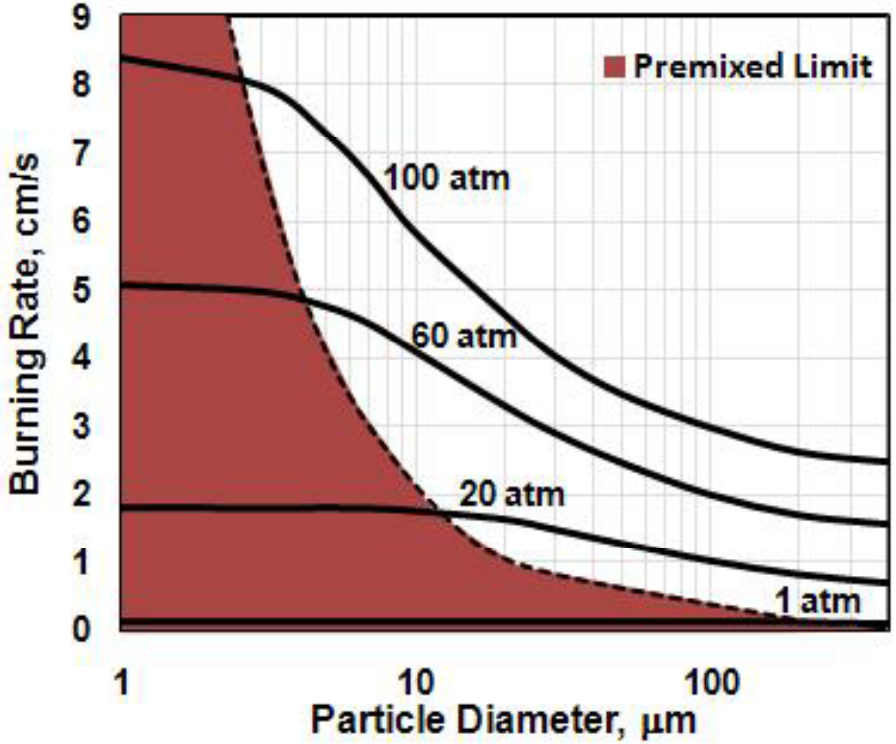

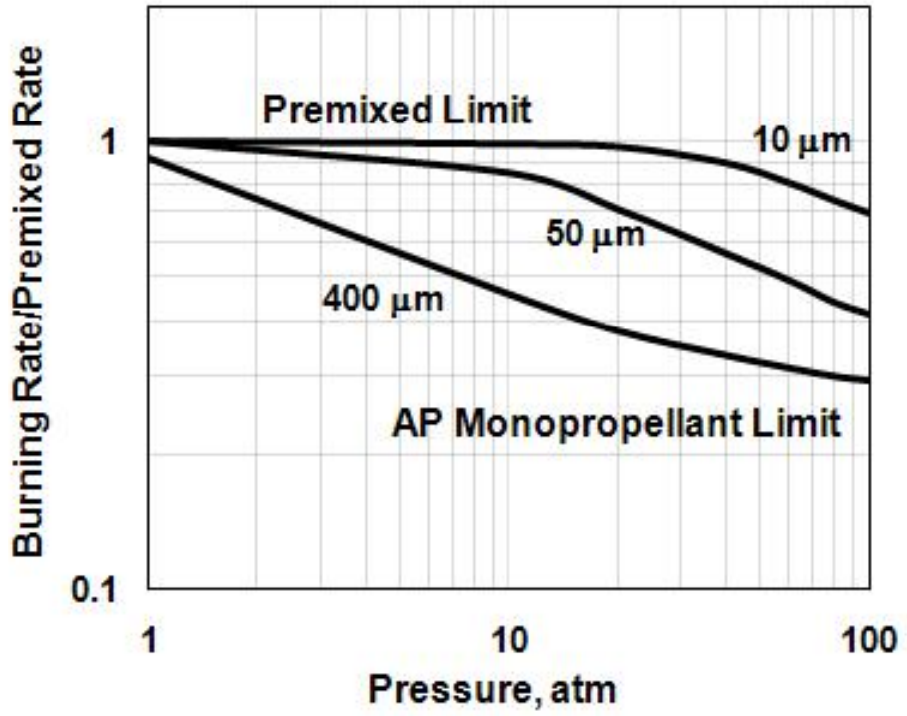

- Premixed limit represents maximum rate for given AP%
- Burning rate vs. particle size curve shifts up and to the left
- Premixed cutoff size decreases with pressure
  - %AP in homogenized binder decreases with pressure

From M.L. Gross and M.W. Beckstead, Comb. Flame 157 (2010) 864

3D Modeling of Heterogeneous Propellants

- Over the past two decades, parallel computing has become a staple of engineering calculations, with multidimensional simulations of heterogeneous propellants following this trend
- Jackson and Buckmaster carried out first three dimensional simulation of solid propellant in 2000
- Random packing algorithms are used to generate the microstructure of a heterogeneous propellant and an unsteady solid gas numerical code for the combustion problem

Random Packing Algorithm for Generating Realistic Microstructures

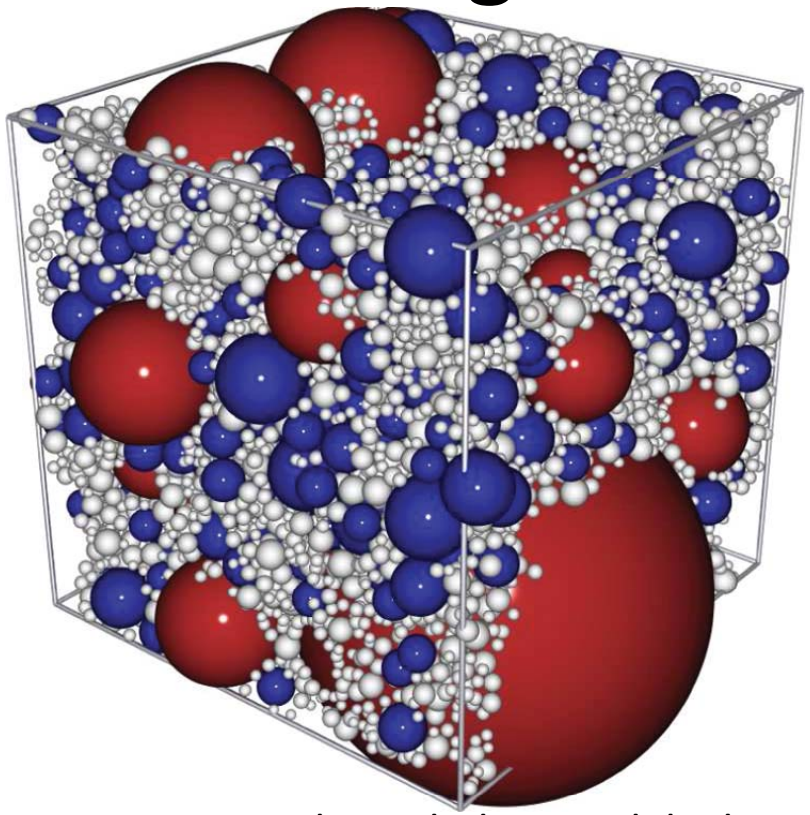

A number of random packing algorithms have been developed for energetic materials (see T.J. Jackson, AIAA Journal 50, 5 (2012) 993.)

Validation of the packing codes are carried out by comparing first-order (volume fraction) and second order statistics to those of surrogate propellants as well as actual AP based propellants using x-ray tomography

- 10,002 particle pack that models the Miller M24 pack (R.R. Miller, AIAA 1982-1096)
- Gray spheres have diameters in the range 5-15 μm, blue spheres have diameters 16-42 μm, and red spheres have diameters 46-211 μm
- Void regions correspond to binder
- Domain is cubic with periodic boundaries, and only those particles with centers inside cube are shown

From T.L. Jackson, AIAA Journal 50, 5, May 2012, 993

Chemistry for Heterogeneous Propellants

- The inclusion of elementary kinetics (hundreds of species) for the gas-phase is well beyond the scope of today's most powerful supercomputers; and the condensed phase chemistry remains generally poorly understood
- Simple global kinetic schemes are adopted, and the challenge is identification of the appropriate parameters for the kinetics
- In the context of AP/HTPB propellants, a three step model, familiar from the BDP model is used, characterized by an AP diffusion decomposition flame, primary diffusion flame, and secondary diffusion flame

$$AP \xrightarrow{R_1} P_d \ \text{(AP products)}$$
$$AP + HTPB \xrightarrow{R_2} P_{pdf}$$
$$HTPB + P_d \xrightarrow{R_3} P_{sdf}$$

- Based on the 2D single particle AP/HTPB modeling results, the mechanism was modified to a 4-step reaction that included a premixed binder flame above the homogenized AP/HTPB mixture

From T.L. Jackson, AIAA Journal 50, 5, May 2012, 993
Gross et al. Comb. Flame 160 (2013) 982

Premixed Binder

- Assume fine AP and HTPB form homogeneous mixture
  - Experimentally supported
  - AP/HTPB react in premixed, laminar reaction zone
  - Limits numerical resolution (Shorter runtime)

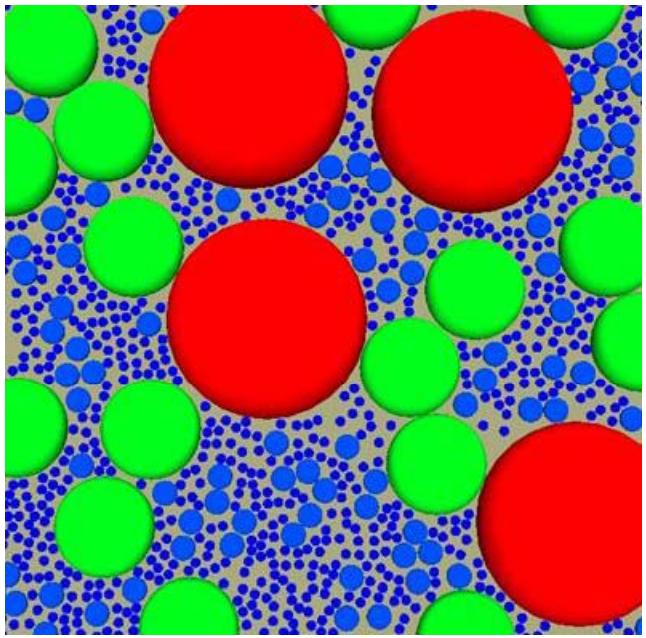

Full pack

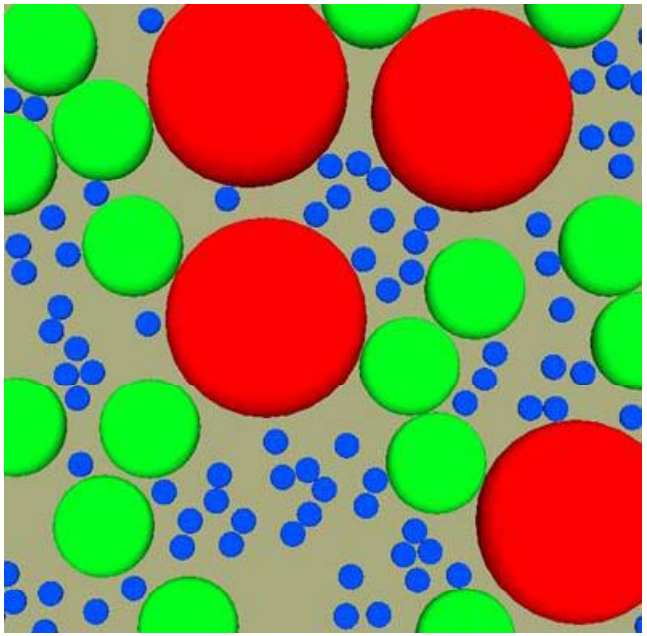

Homogenized pack

AP/HTPB composite propellant burning as a function of pressure

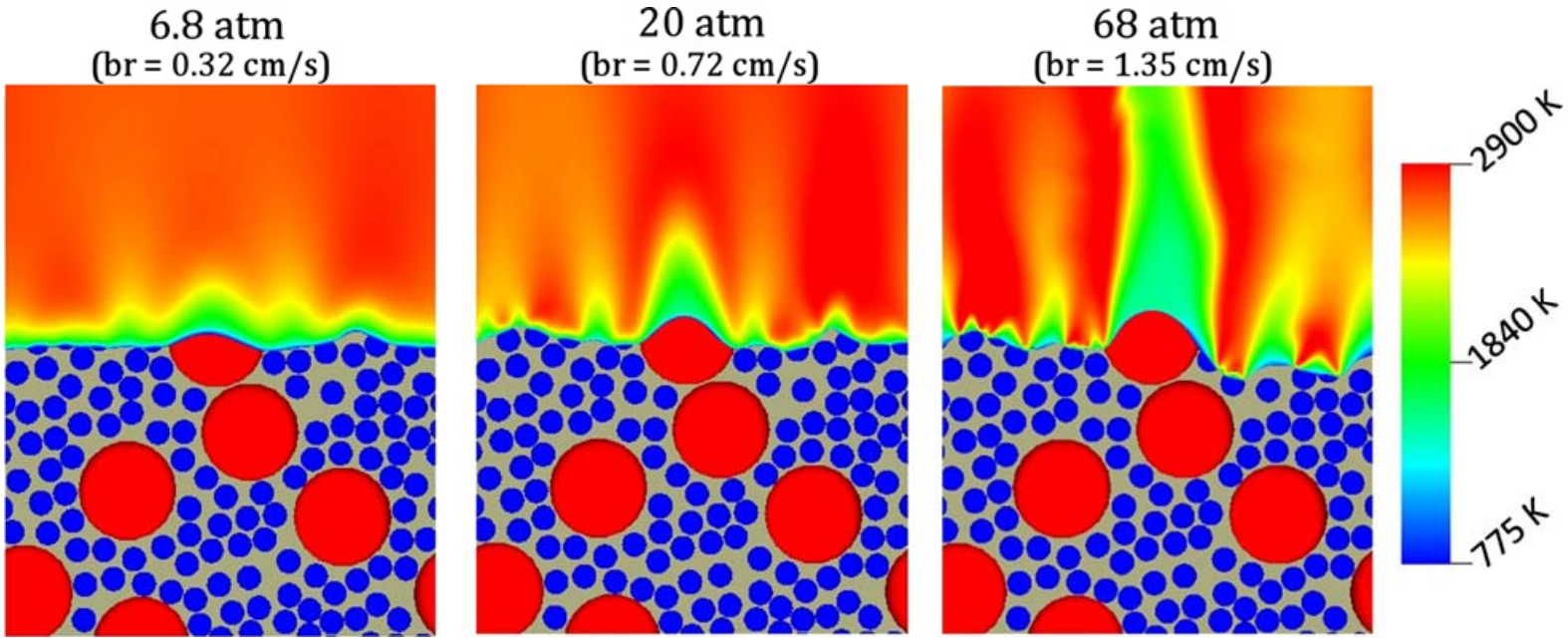

As pressure increases, the premixed flames draws closer to the surface, resulting in a faster burning rate, and the stand-off distance of the diffusion flame increases, decreasing the flame's contribution to burning rate and increasing the surface topology

From Gross et al. Comb. Flame 160 (2013) 982

Surface topography and temperature level surfaces for a sample 3D propellant burning at 20 atm

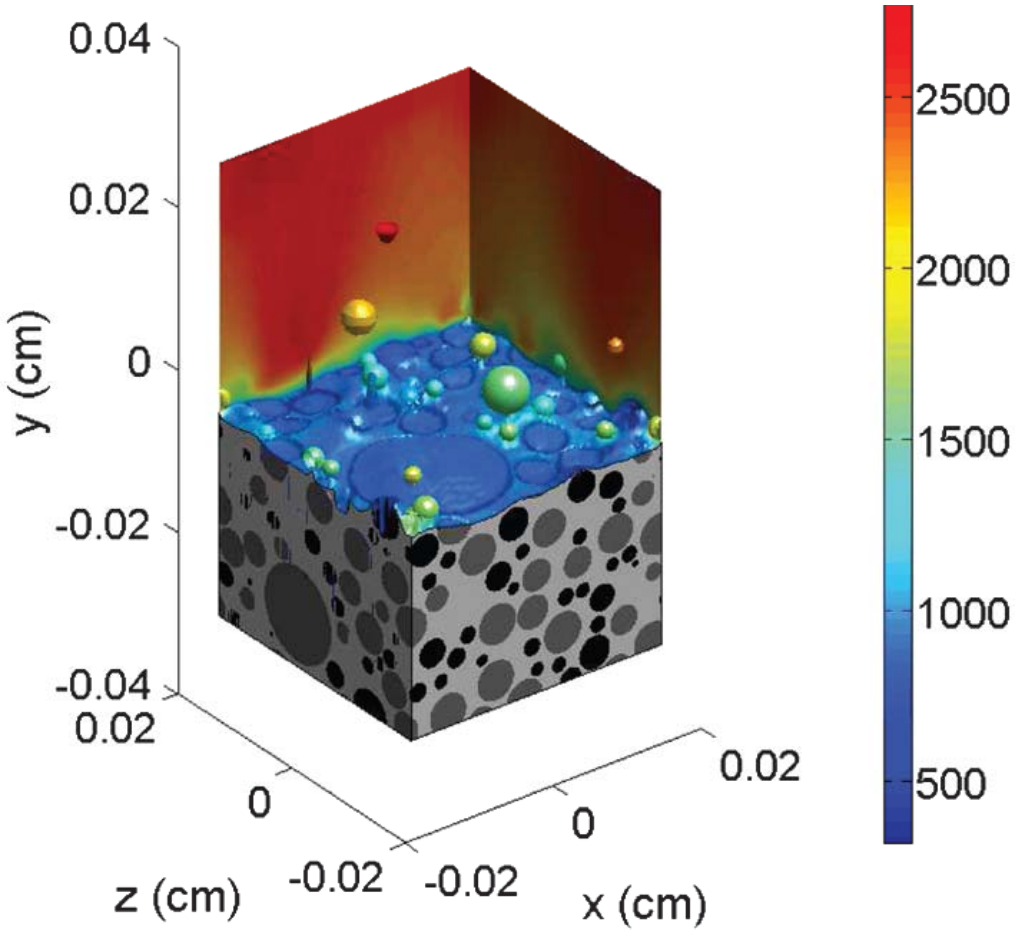

Shown is the instantaneous 3D combustion field for an 18 wt% Al, 54wt% AP propellant

The spheres above the propellant surface are aluminum particles, colored according to their surface temperatures

For submicron aluminum, modeling has been performed where the submicron aluminum is homogenized into the binder

- Studies with aluminum particles are limited
- Studies are necessary that consider surface tension, ignition, phase change, agglomeration, collision, sintering, radiation for proper understanding

From T.L. Jackson, AIAA Journal 50, 5, May 2012, 993